AGU PUBLICATIONS

Geochemistry, Geophysics, Geosystems

RESEARCH ARTICLE
10.1002/2017GC007099

Special Section:
The Arctic: An AGU Joint Special Collection

Significance of Northeast-Trending Features in Canada Basin, Arctic Ocean

D. R. Hutchinson[1], H. R. Jackson[2], D. W. Houseknecht[3], Q. Li[2], J. W. Shimeld[2], D. C. Mosher[2], D. Chian[2], R. W. Saltus[4,5], and G. N. Oakey[2]

[1]U.S. Geological Survey, Woods Hole Science Center, Woods Hole, MA, USA, [2]Geological Survey of Canada Atlantic, Dartmouth, NS, Canada, [3]U.S.Geological Survey, Reston, VA, USA, [4]U.S. Geological Survey, Denver, CO, USA, [5]Now at Cooperative Institute for Research in Environmental Sciences at University of Colorado Boulder, Boulder, CO, USA

Abstract Synthesis of seismic velocity, potential field, and geological data from Canada Basin and its surrounding continental margins suggests that a northeast-trending structural fabric has influenced the origin, evolution, and current tectonics of the basin. This structural fabric has a crustal origin, based on the persistence of these trends in upward continuation of total magnetic intensity data and vertical derivative analysis of free-air gravity data. Three subparallel northeast-trending features are described. Northwind Escarpment, bounding the east side of the Chukchi Borderland, extends ~600 km and separates continental crust of Northwind Ridge from high-velocity transitional crust in Canada Basin. A second, shorter northeast-trending zone extends ~300 km in northern Canada Basin and separates inferred continental crust of Sever Spur from magmatically intruded crust of the High Arctic Large Igneous Province. A third northeast-trending feature, here called the Alaska-Prince Patrick magnetic lineament (APPL) is inferred from magnetic data and its larger regional geologic setting. Analysis of these three features suggests strike slip or transtensional deformation played a role in the opening of Canada Basin. These features can be explained by initial Jurassic-Early Cretaceous strike slip deformation (phase 1) followed in the Early Cretaceous (~134 to ~124 Ma) by rotation of Arctic Alaska with seafloor spreading orthogonal to the fossil spreading axis preserved in the central Canada Basin (phase 2). In this model, the Chukchi Borderland is part of Arctic Alaska.

Plain Language Summary Many models have been proposed to describe the geologic history of Canada Basin, Arctic Ocean, a remote area of Earth where data collection is hampered by perennial ice cover. Our paper merges new geophysical (primarily seismic) data from the basin that was previously published in 2016 with existing gravity, magnetic, and known geology from samples to propose that (a) a northeast-trending structural fabric exists in the basin, and (b) this fabric arises from strike-slip or transtensional motion during basin formation. This new model has many testable attributes.

Key Points:
- Three northeast-trending linear structural zones of roughly 300 to >1,000 km exist in Canada Basin.
- These zones suggest the importance of a long-lived strike slip or transtensional fabric in the evolution of Canada Basin.
- A two-phase model is proposed in which rifting with large strike-slip components is followed by a change in deformation direction with rotational seafloor spreading.

Correspondence to:
D. Hutchinson,
dhutchinson@usgs.gov

Citation:
Hutchinson, D. R., Jackson, H. R., Houseknecht, D. W., Li, Q., Shimeld, J. W., Mosher, D. C., . . . Oakey, G. N. (2017). Significance of northeast-trending features in Canada Basin, Arctic Ocean. *Geochemistry, Geophysics, Geosystems*, *18*, 4156–4178. https://doi.org/10.1002/2017GC007099

Received 29 JUN 2017
Accepted 23 OCT 2017
Accepted article online 1 NOV 2017
Published online 28 NOV 2017

1. Introduction

The deep-water Canada Basin of the Arctic Ocean (Figure 1), covered by year-round ice until recently, has closely guarded the secrets of its geologic past. Without data to constrain interpretations, many models have been proposed to explain how the basin formed. Early models of oceanization of the continental crust (Shatsky, 1935) or capture of Paleozoic or Cretaceous ocean crust from the Pacific (Churkin & Trexler, 1980) have generally been discounted. Weak linear magnetic anomalies (Gaina et al., 2011; Vogt et al., 1982) and a bent, elongated negative gravity anomaly traversing Canada Basin (Grantz et al., 1979; Laxon & McAdoo, 1994; Taylor et al., 1981) have been interpreted as evidence of seafloor spreading and a fossil spreading center, respectively. These potential field data, integrated with geologic mapping showing widespread rifting and geologic similarities along the Alaskan and Canadian margins, have led to a consensus model in which Alaska and Arctic Canada are conjugate margins that rotated apart in Early Cretaceous time after a prolonged period of extension (Carey, 1955; Cochran et al., 2006; Døssing et al., 2013; Grantz et al., 1979, 1990b, 1998, 2011; Tailleur, 1973). Biostratigraphic evidence from onshore wells has been used to reconstruct Point Barrow on the Alaskan margin (Figure 1) to the southern portion of Prince Patrick Island on the Canadian margin (Embry, 1990; Mickey et al., 2002). Zircon geochronology further supports a common geologic heritage of Paleozoic rocks underlying the Alaskan and Canadian margins (Gottlieb et al., 2014). Similarities in seismic stratigraphy and interpreted deformation support this rotational closure (Houseknecht & Connors,

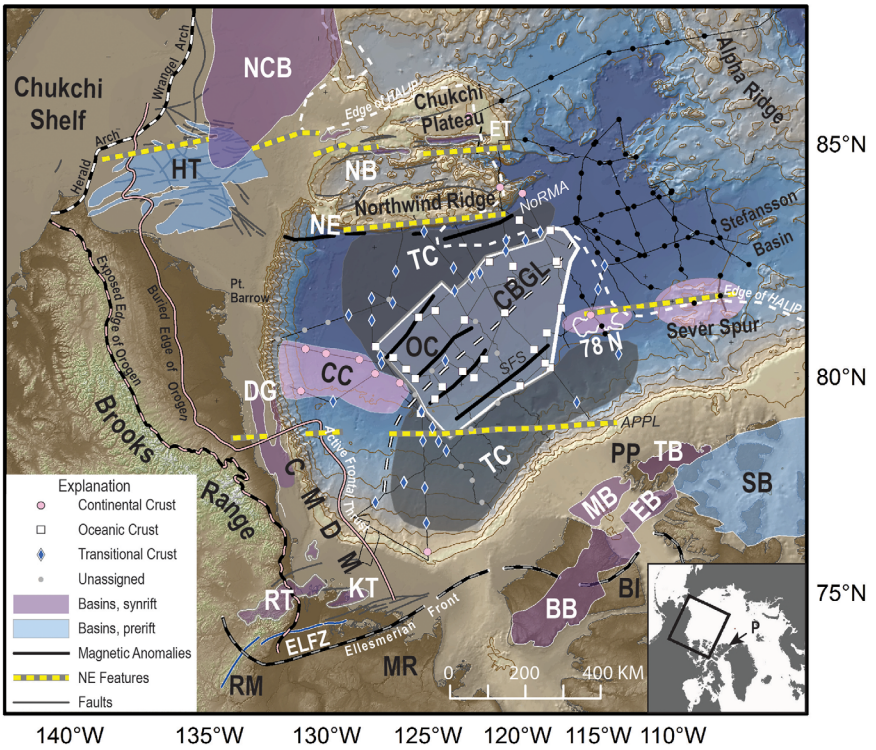

Figure 1. Map of the Canada Basin and vicinity showing features described in this paper. Thin solid black lines show seismic reflection data locations. Sonobuoy results from Chian et al. (2016) use symbols shown in the Explanation except for small black dots (HALIP) not interpreted as part of Chian et al. (2016). Symbols correspond to shading for: OC, oceanic crust in white; TC, transitional crust in dark gray; CC, continental crust in pink. The pink ellipses of continental crust shown near 78 N and Sever Spur are approximate, as only one sonobuoy solution exists. Dashed white line with black outline—CBGL (Canada Basin Gravity Low) anomaly. Yellow-gray dashed lines show features discussed in the text. Names of the rift basins are TB, MB, EB, and BB (Tullett Basin, M'Clure Strait Basin, Eglinton Basin, and Banks Basin, respectively, adapted from Miall, 1976, and Harrison and Brent, 2005), NCB and DG (North Chukchi Basin and Dinkum Graben, respectively, mapped for this study), 78 N, ET, RT, KT (78 N Basin, Egiazarov Trough, Richardson Trough, and Kugmallit Trough respectively, approximated using the −50 mgal contour from Figure 4a), NB—Northwind Basin shown as a bathymetry depression. Prerift basins are labeled as SB (Ellesmerian Sverdrup Basin; Harrison & Brent, 2005) and HT (Ellesmerian Hanna Trough, mapped for this study). Other abbreviations: NE, Northwind Escarpment; CMDM, Canning Mackenzie Deformed Margin; BI, Banks Island; PP, Prince Patrick Island; MR, Mackenzie River; P (inset map), Pearya. Dashed black-rose line—surface location of Brooks Range deformation front (Houseknecht & Bird, 2011); solid rose line—buried edge of Brooks Range deformation (Houseknecht & Bird, 2011), gray lines—faults (Garrity & Soller, 2009); blue line with white outline—ELFZ, Eskimo Lakes fault zone; gray/black dashed line—Ellesmerian Front (adapted from Lane and Dietrich, 1995, and Gottlieb et al., 2014); dashed white-black line—Herald-Wrangel Arch (mapped for this paper). Projection is polar stereographic with a central meridian of 90°W and standard parallel of 75°N.

2016). Recently acquired seismic reflection and refraction data from the Canada Basin (Chian et al., 2016) and plate reconstruction models (Amato et al., 2015; Doré et al., 2016; Miller et al., 2017; Shephard et al., 2013) are generally consistent with the rotational opening model.

The rotational model is not universally accepted, however, and a wide variety of alternative models exist (Lane, 1997; Lane et al., 2015, Lawver & Scotese, 1990). A problem with many opening models, and particularly the rotational model, is explaining the location and shape of Chukchi Borderland, a submerged marginal plateau north of Alaska consisting of the Chukchi Plateau, Northwind Ridge, and internal basins. When reconstructed, the borderland overlaps the Canadian Arctic Islands, requiring unique complexities to avoid the overlap (e.g., Amato et al., 2015; Doré et al., 2016; Grantz et al., 1998, 2011; Lawver & Scotese, 1990; Shephard et al., 2013). Recent detrital zircon analyses have linked Chukchi Borderland to Ellesmere Island (O'Brien et al., 2016) or more broadly to Caledonian rocks further north (Brumley et al., 2015). Complicating any tectonic interpretation is the presence of the Alpha-Mendeleev Ridge System and its associated High Arctic Large Igneous Province (HALIP; Døssing et al., 2013; Maher, 2001; Oakey & Saltus, 2016; Saltus et al.,

2011). The strong magnetic signature of HALIP dominates the northern Canada Basin, obscuring possible preexisting connections between features of Canada Basin and Eurasia.

The crustal velocity mapping presented in Chian et al. (2016) provides new constraints for integrating existing geological and geophysical data. In attempting such an integration, we emphasize the existence of northeast-trending features in the basin. This paper characterizes these features within and on the edges of Canada Basin, as well as features on land in Alaska and Canada. Following a description of the data sets used, we synthesize our observations with the crustal results of Chian et al. (2016) and finally propose that the most likely explanation for this trend is an inherited subparallel fabric indicative of widespread strike slip, or transtensional, tectonics in the early formation of the basin. We propose a two-phase model of opening in which development of these strike-slip features in the latest Jurassic to Early Cretaceous (phase 1) preceded seafloor spreading and rotation in the Early Cretaceous (phase 2). The ideas in this paper lead to testable hypotheses.

2. Geologic Framework

Canada Basin is a small ocean basin bordered on the south and east by the Arctic continental margins of Alaska and Canada respectively, and on the west and north by large submerged bathymetric complexes, Northwind Ridge of Chukchi Borderland and Alpha Ridge respectively (Figure 1). The Alaskan and Canadian Arctic margins are sediment covered passive continental margins, although extant tectonic impingement associated with the northeast Brooks Range deforms the margin from northeastern Alaska to the Mackenzie River delta (Grantz et al., 1990a; Helwig et al., 2011; Houseknecht & Bird, 2011).

In the deep water of Canada Basin, velocities mapped from sonobuoys using seismic refraction forward modeling (Chian et al., 2016) indicate that oceanic crust, characterized by oceanic layer 3 velocities of 6.7–7.1 km/s, is restricted to the central portion of the basin (white squares, Figure 1). Transitional crust, characterized by higher velocities of 7.2–7.6 km/s, in general surrounds the polygon of oceanic crust, but varies considerably in width, $>$350 km in the wide southeastern portion of the basin beneath the Mackenzie Fan north of the Mackenzie River (MR, Figure 1) to $<$40 km in a narrow zone offshore northern Alaska (blue diamonds, Figure 1). Transitional crust is inferred either to be serpentinized mantle from its association with the nonmagmatic margins around the southeastern Canada Basin, or to be underplated or intruded gabbroic material for the areas along Northwind Ridge and in northern Canada Basin from their proximity to the distinct high-amplitude magnetic anomalies of HALIP. Thinned continental crust, characterized by basement and crustal velocities $\leq$6.6 km/s, is least sampled in this mapping, but also occurs on three sides of the basin (pink circles, Figure 1): beneath Northwind Ridge, within a large block that extends more than 300 km north of the Alaskan continental margin (CC, Figure 1), and within a buried graben in the northeast Canada Basin (78 N, Figure 1). The CC block of continental crust coincides with the offshore extension of the D3 magnetic domain of Saltus et al. (2011).

Crustal velocity mapping (Chian et al., 2016) and sediment thickness data (Shimeld et al., 2016) also demonstrate that the polygon of oceanic crust is bisected by the Canada Basin Gravity Low anomaly (CBGL, Figure 1). The CBGL is associated with a roughly 45 km wide valley with high-relief basement blocks along its axis (Shimeld et al., 2016). The velocity data are therefore consistent with the interpretation of the CBGL as an extinct spreading center (Grantz et al., 1979; Laxon & McAdoo, 1994), possibly of slow or ultraslow speed where pronounced central valleys are best preserved (Dick et al., 2003). Where the CBGL bends toward the Mackenzie River along the Canadian margin, the velocity data do not show the existence of oceanic crust, but rather show transitional crustal velocities. The high velocities of the southern extension of the CBGL were interpreted as serpentinized mantle, possibly created by nonmagmatic rifting (Chian et al., 2016).

While the Alaskan and Canadian Arctic island margins are generally considered to be passive continental margins (Dixon & Dietrich, 1990; Grantz et al., 1990a), a segment of the margin is deforming with diffuse seismicity and shows large upright folds in the youngest subsurface sediments (Grantz et al., 1990a, 2011; Helwig et al., 2011; Houseknecht & Bird, 2011; Sippel et al., 2013). This deformation zone has been termed the Barter Island sector (Grantz & May, 1982; Grantz et al., 1990a), the Beaufort Foldbelt (Helwig et al., 2011) and more recently the Canada-Mackenzie Deformed Margin, (CMDM, Figure 1) (Houseknecht & Bird, 2011). We use the CMDM terminology and active deformation front of Houseknecht and Bird (2011) in this paper (solid rose-colored line in Figure 1).

3. Data Sets

In order to identify regional tectonic trends, bathymetry, magnetic, gravity, seismic reflection, and geological data have been integrated with the recent refraction results of Chian et al. (2016). In this section, we describe the data sets and selected features used in our analysis that have been mapped or described by others.

3.1. Multibeam Bathymetric Data

Multibeam bathymetric data have sometimes provided the first accurate views of seafloor morphology in parts of the Canada Basin and allow contouring seafloor relief at 100 m or higher resolution (IBCAO 3 map of Jakobsson et al., 2012). We use the contour spacing of 100 m isobaths along slopes to define linear trends of bathymetric and topographic features (Figure 2).

3.2. Magnetic Data

Magnetic domains mapped by Saltus et al. (2011) are shown on the magnetic map of Gaina et al. (2011) as areas encircled by dashed lines and labeled with letters (B, D, F) and numbers (Figure 3a). These domains were classified according to magnetic character and interpreted by their magnetic fabric, association with regions classified with different crustal character, and correlation with gravity anomalies. The most prominent domain is F1, a region of chaotic magnetic anomalies called the High Arctic Magnetic High Domain, which is a subset of the High Arctic Large Igneous Province or HALIP (Døssing et al., 2013; Maher, 2001; Oakey & Saltus, 2016). We use the term HALIP in this paper to recognize its larger areal extent. HALIP is associated with mafic rich and locally underplated or intruded crust (Funck et al., 2011). The D-anomalies represent deep magnetic highs of more localized extent than the anomalies associated with the HALIP, but, like the HALIP, have significant mafic components in the crust. The B3 domain is associated with deformed magnetic regions, in this case, the Brooks Range orogenic belt. Most of the Canada Basin and the continental margins were classified as an undifferentiated C domain (Saltus et al., 2011) but can now be subdivided into oceanic, transitional, and continental crust based on the results of Chian et al. (2016). The linear magnetic anomalies, interpreted to be part of seafloor spreading anomalies (Chian et al., 2016; Grantz et al., 2011; Taylor et al., 1981; Vogt et al., 1982), are shown by black lines labeled SFS (Figure 3a).

To further investigate magnetic sources, the magnetic data of Gaina et al. (2011) were processed in the Fourier domain with the fast Fourier transformation (FFT). As a widely used data processing method for potential field data (e.g., Blakely, 1996), the upward continuation of potential field data is a stable low-pass filtering process for extracting deeply buried geological objects by depressing the higher-frequency anomalies associated with shallow bodies. The vertical derivative of the data makes it possible to extract geological/geophysical boundaries at different depths. The magnetic data were first upward continued from 2 km (cell size of potential field raster grids used in this paper) to 200 km in 1 km steps. In a subsequent step, the first and second vertical derivatives were calculated using the georeferenced GeoTiff raster in the ArcGIS environment. The vertical derivative method is a high-pass filtering process that outlines geological and/or geophysical boundaries by enhancing short wavelength signals. In addition to the starting magnetic anomaly grid (Figure 3a), we show the 4 km (Figure 3b) and the first derivative of the 150 km upward continued data (Figure 3c). The 4 km upward continued data remove shallow, near-surface anomalies. The first derivative of the 150 km upward continued data show source anomalies in the lower crust.

3.3. Gravity Data

Gravity data from the ARCS-2 altimetric satellite compilation of McAdoo et al. (2013) are used (Figure 4a) to show the Canada Basin Gravity Low (CBGL) anomaly of Laxon and McAdoo (1994), as well as the shelf-edge paired gravity anomalies (SEPA) described by Vogt et al. (1998).

The gravity data were also processed in the Fourier domain to produce a vertical derivative map (Figure 4b) and an 8 km upward continued map (Figure 4c). Shallow or short wavelength signals, interpolation artifacts, or even noise can sometimes affect vertical derivative maps. The upward continued data can both reduce these artifacts and also delineate deeper density objects and their spatial boundaries.

3.4. Multichannel Seismic Reflection Data

High-resolution multichannel seismic reflection data collected collaboratively by Canada and the United States between 2007 and 2011 (Mosher et al., 2013, 2016) are used to illustrate the subsurface geometry of trends otherwise identified in the bathymetry or potential field data (Figures 5 and 6) Acquisition and

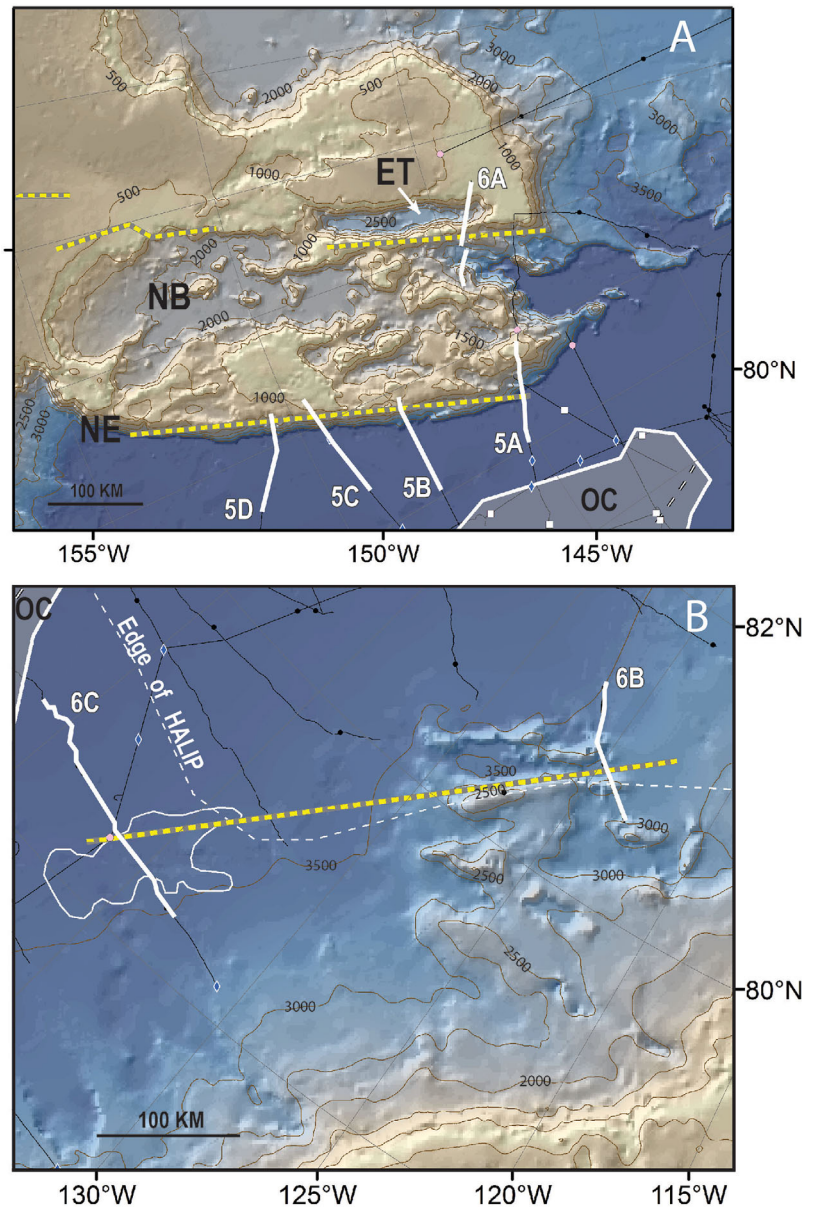

Figure 2. Bathymetry detail of Chukchi Borderland and Sever Spur. Prominent subparallel north, northeast striking features (yellow-gray dashed lines), oceanic crust (OC), 78 N Basin (thin white line in Figure 2b), and edge of HALIP (dashed white line in Figure 2b) are from Figure 1. (a) Detailed bathymetry of Chukchi Borderland showing location of Egiazarov Trough (ET) and locations of seismic figures (white lines). (b) Detailed bathymetry of Sever Spur showing locations of seismic lines on Sever Spur and 78 N basin (white lines). See Figure 1 for additional explanation.

processing of these data are given in Mosher et al. (2013). Additional multichannel seismic data located on the Chukchi Plateau are used (Figure 6a) (Coakley et al., 2005).

3.5. Geological Data

Geological trends are taken from the Geological Map of North America (Garrity & Soller, 2009), the Geological Map of the Arctic (Harrison et al., 2011), the domains mapped by Houseknecht and Bird (2011), and boundaries mapped from our interpretation of seismic data both offshore in the Canada Basin and onshore in Alaska and Canada. Several large geological structures have been mapped onshore (Figure 1), such as the surficial and buried deformation fronts of the Brooks Range (rose-colored dashed and rose-colored solid lines, respectively, Figure 1) from Houseknecht and Bird (2011). Although the topography of the Brooks

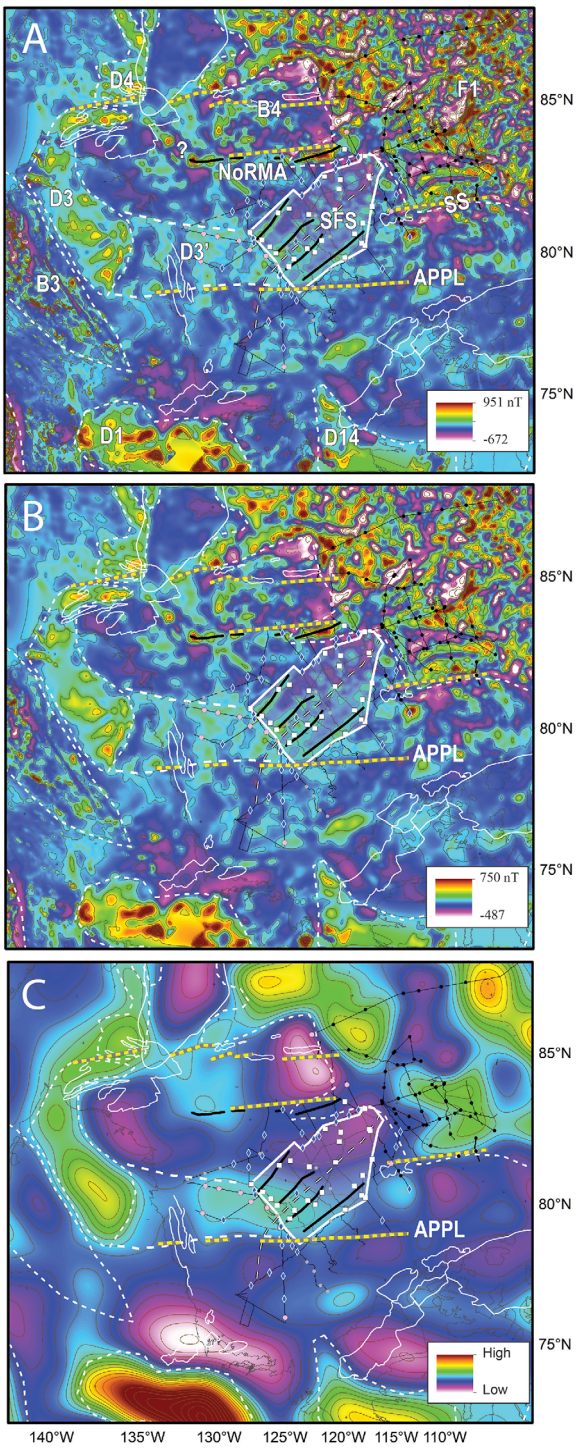

Figure 3. Magnetic anomaly maps of the study area. Northeast-trending features (yellow-gray dashed lines), basins (thin white lines), area of oceanic crust (heavy white line), and seafloor spreading anomalies (heavy black lines) are from Figure 1. (a) magnetic anomaly map from Gaina et al. (2011) showing magnetic domains (B3, B4, D1, D3, D4, D14, F1, dashed white lines) interpreted by Saltus et al. (2011) and explained in the text. D3′, offshore extension of magnetic domain D3 (described in Chian et al., 2016); NoRMA, Northwind Ridge Magnetic Anomaly; SFS, Seafloor spreading magnetic anomalies; APPL, Alaska-Prince Patrick magnetic Lineament; SS, Sever Spur. (b) Magnetic anomaly map (Figure3a) with an upward continuation filter to 4 km. Magnetic domain boundaries are from Figure3a. (c) First vertical derivative map of magnetic anomaly map (Figure 3a) with an upward continuation filter to 150 km. Magnetic domain boundaries are from Figure3a. See Figure 1 for additional explanation.

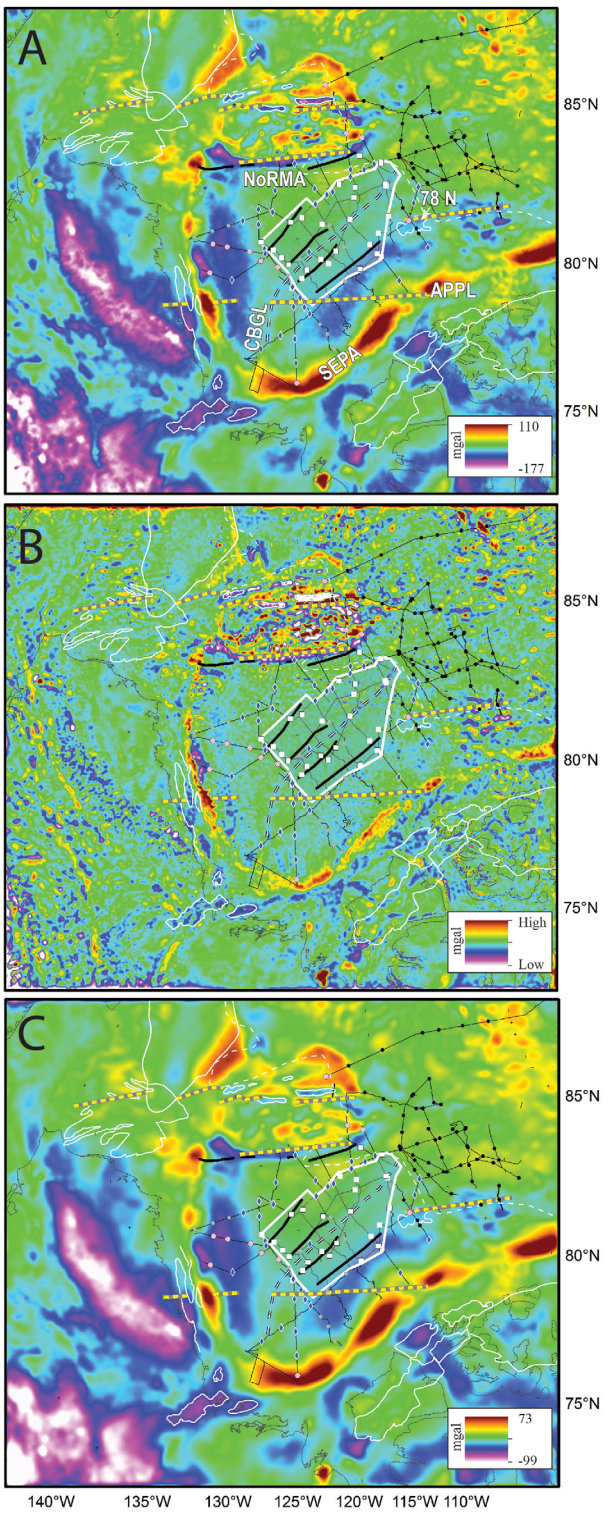

Figure 4. Free-air gravity anomaly maps of the study area. Northeast-trending features (yellow-gray dashed lines), basins (thin white lines), area of oceanic crust (heavy white line), and seafloor spreading anomalies (heavy lack lines) are from Figure 1. (a). Free-air gravity anomaly map from McAdoo et al. (2013). Gravity anomaly abbreviations: CBGL, Canada Basin Gravity Low; 78 N, outline of 78 N basin gravity anomaly; SEPA, shelf edge paired anomaly. Magnetic anomaly abbreviations: NoRMA, Northwind Ridge Magnetic Anomaly, APPL, Alaska-Prince Patrick lineament. (b) First vertical derivative of Figure 4a. (c) Free-air gravity anomaly map (Figure 4a) with an upward continuation filter to 8 km. See Figure 1 for additional explanation.

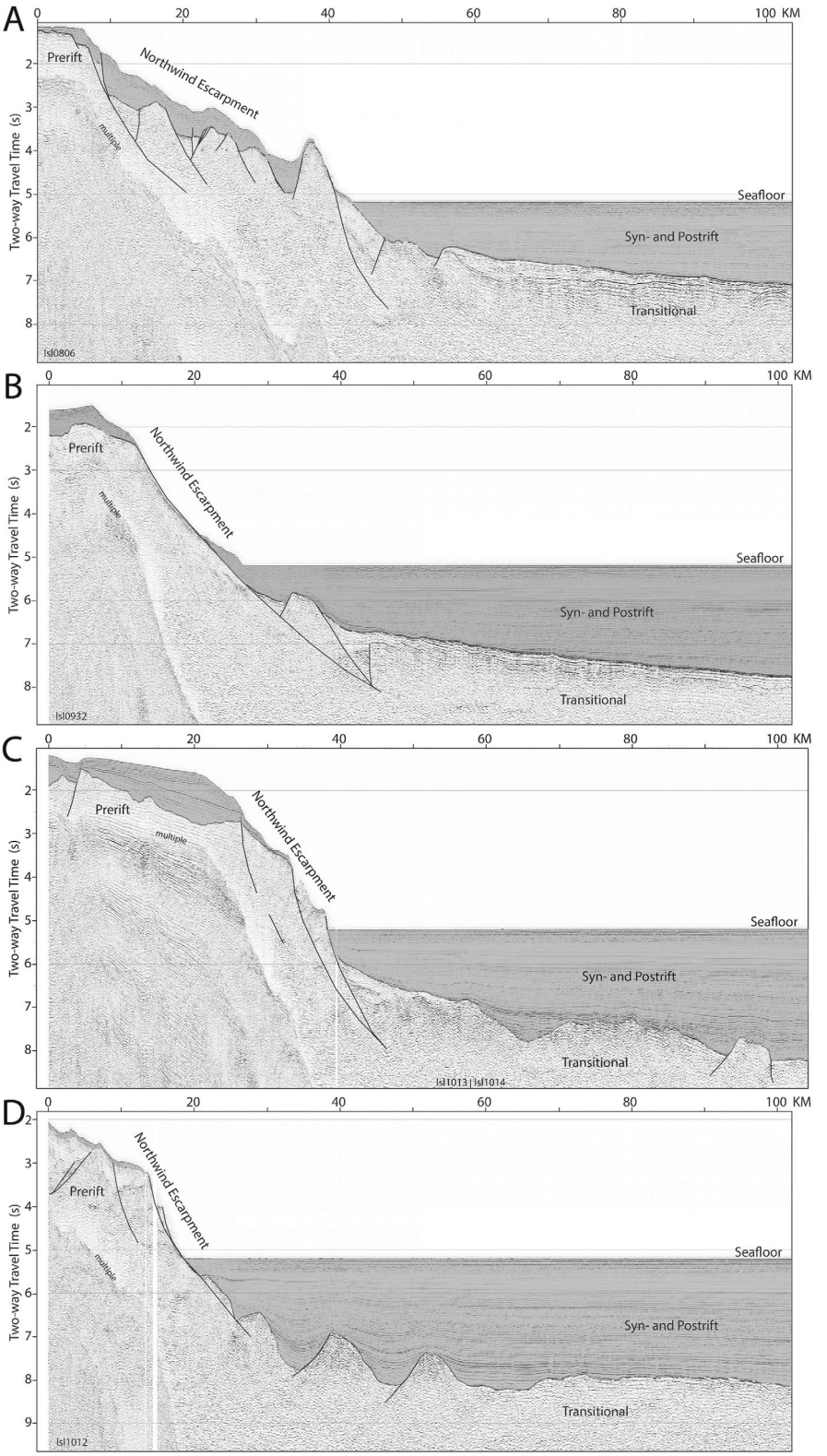

Figure 5. Seismic profiles across Northwind Escarpment from north to south showing tilted and truncated strata at the top of the escarpment, faulting along the escarpment, and the absence of large synrift structures at the base of the escarpment. HALIP magmatism may obscure faulting and stratigraphic reflections at the base of Northwind Escarpment. Locations are shown in Figure 2a. Gray shading shows postrift and possible synrift sedimentary deposits. (a) Line lsl0806. (b). Line lsl0932. (c). Combined lines lsl1013 and lsl1014. (d) Line lsl1012.

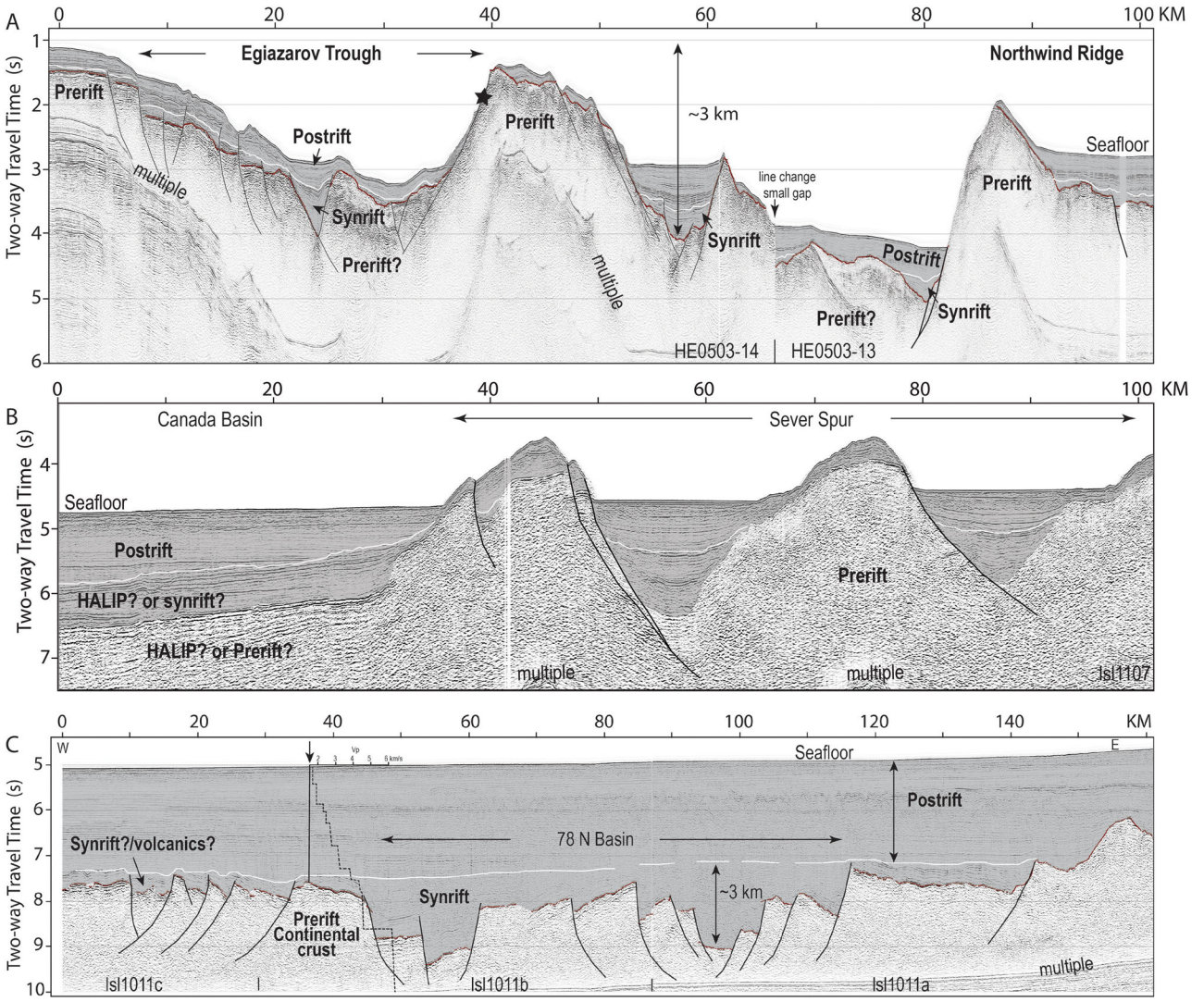

Figure 6. Seismic profiles on Chukchi Borderland, Sever Spur, and 78 N basin. Locations are shown in Figure 2. Gray shading shows postrift and inferred synrift sedimentary deposits, separated by a thin white line along the interpreted postrift unconformity. (a) Combined line HE0503-13 and HE0503-14 located at the north end of the Central Chukchi Basin and Northwind Ridge. (b). Line lsl1107 located on Sever Spur showing similar relations as seen on Northwind Escarpment (Figure 5), i.e., tilted and truncated sediments along the tops of ridges and the absence of large synrift (tilted, fanning strata) at the base of the ridges. Scale is same as Figure 6a. (c) Combined lines lsl0811a, lsl0811b, and lsl0811c that cross the 78 N basin. Note scale change for this profile, with horizontal and vertical scales at same aspect ratio, but compressed; deeper units are thinner and basement offsets are less at higher velocities in travel time sections compared to their true relative thicknesses and offsets in a depth section. Arrow indicates the location of sonobuoy 2009-28-1 (Chian & Lebedeva, 2015), and the resulting Vp solution plotted relative to the sonobuoy location. Velocities increase from 6.4 (inferred continental crust) to 8.0 km/s (upper mantle, not illustrated at this scale) at ~10.5 s two-way travel time and is the basis for interpreting a continental block beneath the 78 N basin.

Range trends obliquely toward the northern Alaskan coast, the deformation front is notable for its abrupt northerly bend relative to the surficial trace of the mountain range. The bend, or northeast-trending, part of the deformation front is called the Canning deformed zone (Grantz et al., 1991) and forms the western limit of major Paleogene to late Quaternary uplift, diffuse seismicity, and counter-clockwise rotation of the Brooks Range relative to its general east-west orientation (Grantz & May, 1982; Grantz et al., 1990a; Lane & Dietrich, 1995). Approximately 575 km further east, a counterpart to the Canning deformed zone is the Richardson dextral strike-slip zone which coincides with the Richardson Mountains (RM, Figure 1) (Grantz et al., 1990a; Mazzotti & Hyndman, 2002), the Richardson Trough (RT, Figure 1), Kugmallit Trough (KT, Figure 1), and possibly the Eskimo Lakes Fault zone (ELFZ, Figure 1) (Graves et al., 2010; Helwig et al., 2011; Houseknecht & Bird, 2011). Together, these features broadly define the eastern extent of Brooks Range deformation along the Beaufort margin.

The Dinkum Graben of Grantz and May (1982) is interpreted from seismic reflection data to be a Jurassic-aged rift basin oriented parallel to the central Alaskan continental margin (DG, Figure 1). East of 145°W, the graben is masked by a thick cover of deformed Cenozoic strata (Grantz et al., 1990b; Houseknecht & Bird, 2011), although recent mapping has identified parts of the graben further east within the CMDM (Houseknecht & Connors, 2015).

Additional buried or exposed Jurassic and younger rift basins have been identified in Canada, (TB, MB, EB, BB, KT, and RT, Figure 1) The orientations of these basins are generally controlled by the underlying Ellesmerian tectonic fabric (Graves et al., 2010; Harrison & Brent, 2005; Miall, 1976). Several gravity lows that could locate as yet unnamed rift basins on the Chukchi Borderland are shown by the −50 mgal gravity contour (Figure 1). These gravity lows approximately coincide with synrift basins interpreted on seismic data of Nikishin et al. (2014) and Ilhan and Coakley (2015). The outlines of the larger Northwind and North Chukchi basins (Drachev, 2016; Grantz & May, 1982) are also shown (NB, NCB, Figure 1).

Outcrop of the relatively undeformed Carboniferous to Early Cretaceous strata of the Sverdrup Basin occurs along the northeastern edge of our study area (SB, Figure 1). The north-northwest-trending Hanna Trough (HT, Figure 1) is a basin of Devonian (?) to Late Jurassic age (Kumar et al., 2011; Sherwood et al., 2002). Synrift normal faults of the HT are developed along a north-trending, contractional structural grain in the pre-Mississippian basement rocks (Sherwood et al. 2002). These synrift normal faults were reactivated as wrench faults during the Paleogene Lothamer (1992) and are shown on the Geologic Map of North America (Garrity & Soller, 2009) and in Figure 1 (dark gray lines).

4. Northeast-Trending Features

This section describes northeast-trending features in the Canada Basin identified from integrating the various geophysical data sets.

4.1. Northwind Escarpment

Northwind Escarpment, which forms the eastern edge of Chukchi Borderland, rises 2,000–2,800 m above the flat abyssal seafloor of Canada Basin with slopes generally of 10°–20°, but locally exceeding 50° (Brumley, 2009). The escarpment is one of the dominant morphologic features of Canada Basin, trending northeast for almost 600 km from the Alaska margin (Figures 1 and 2a). Crustal velocities interpreted by Chian et al. (2016) for Northwind Ridge are continental, similar to results obtained in earlier refraction and potential field modeling studies (e.g., Dove et al., 2010; Hall, 1990; Hegewald & Jokat, 2013). The high relative elevation of the Chukchi Borderland is also consistent with lower density continental rocks than with denser transitional and oceanic rocks (Dove et al., 2010; Hall, 1990). Northwind Escarpment is prominently visible in the free-air gravity anomaly as a narrow, elongate, discontinuous negative anomaly (Figure 4a). In both the first vertical derivative of gravity (Figure 4b) and the 8 km upward continued map (Figure 4c), the escarpment is characterized by a narrow, elongate, negative gravity anomaly that separates the large amplitude anomalies of Chukchi Borderland from the subdued anomalies of Canada Basin.

Just east of Northwind Ridge, a high-amplitude positive magnetic anomaly here called the Northwind Ridge Magnetic Anomaly (NoRMA, Figure 3a) exists. The northern-most part of NoRMA is included as part of the Alpha-Mendeleev HALIP in the F1 domain of Saltus et al. (2011) (Figure 3a), but is excluded in the HALIP polygon proposed by Oakey and Saltus, (2016). NoRMA parallels Northwind Escarpment southward with discontinuous, lower amplitude segments, and may even continue southwestward onto the Chukchi Shelf (Figure 3a). The northern part of the NoRMA anomaly is visible in the 4 km upward continued data (Figure 3b) as one of the only positive anomalies in Canada Basin. Both the magnetic anomaly map (Figure 3a) and 4 km upward continued magnetic data (Figure 3b) show the different magnetic character of Chukchi Borderland from NoRMA and the HALIP. In the vertical derivative of the 150 km upward continued data (Figure 3c), NoRMA marks a saddle between a strongly negative anomaly beneath the northern half of the Chukchi Borderland and a less negative magnetic anomaly beneath the northern half of the polygon of oceanic crust (Figure 3c). NoRMA, therefore, is an anomaly well represented with both shallow and deep sources.

Crustal velocities of 7.2–7.3 km/s from the sonobuoys along NoRMA are interpreted as magmatic (gabbroic?) material emplaced during formation of the HALIP (Chian et al., 2016). Basalts dredged from northern Northwind Ridge (Andronikov et al., 2008; Mukasa et al., 2009) support the interpretation that large-

amplitude magnetic anomalies similar to NoRMA and those found in the HALIP (Saltus et al., 2011) could be related to emplacement of basaltic or gabbroic material. Gravity models show an abrupt increase in crustal thickness under Northwind Ridge from thinner values under the Canada Basin (Hall, 1990; Oakey & Saltus, 2016; Chian et al., 2016). Because Northwind Escarpment forms the boundary between the continental rocks of Northwind Ridge and the high-velocity magmatic rocks beneath NoRMA, it is therefore interpreted to represent a first-order crustal boundary along the edge of Canada Basin.

Seismic stratigraphic relations show that Northwind Escarpment coincides with a series of large faults. Strata at the top of the escarpment are tilted and truncated by the inferred faults. (Figures 5b and 5c). It has not been possible to correlate horizons between the top and bottom of the escarpment, although the minimum throw can be constrained by the 2,000–2,800 m offset between the top of Northwind Ridge and the adjacent seafloor of Canada Basin. Previous studies have interpreted Northwind Escarpment as a compressional zone resulting from clockwise rotation of Chukchi Borderland (Doré et al., 2016; Grantz et al., 1998, 2011) or an extensional fault system that is part of a basin and range tectonic regime (Brumley, 2009, 2014). The seismic reflection data crossing the escarpment do not support either of those opposing interpretations. If the fault throw is normal, there is no evidence for large, synrift half grabens at the base of the escarpment in the adjacent Canada Basin. The deeper, older reflections beneath the inferred synrift and postrift strata are discontinuous, subhorizontal, seaward dipping, or do not occur at all (Figures 5a and 5b). These deeper reflections do not show evidence for rotation and thickening into the fault as might be expected for a large normal fault along the edge of an uplifted basement block (Northwind Ridge) with major topographic relief (Figures 5c and 5d). Nor do the strata below the synrift and postrift sediments show major folds, faults, inversions, or other features that might indicate regional contractional structures. Some of the deeper stratigraphic and structural relations may be obscured by HALIP volcanism or be poorly imaged because of limitations of the seismic reflection system. Sediments infilling Canada Basin have an onlap relation on the buried portion of the escarpment, with little or no postdepositional deformation (Figure 5).

We propose that Northwind Escarpment is neither extensional nor compressional but rather represents a dipping strike slip or transtensional fault system. Faults of similar length are known along submerged continental blocks associated with strike-slip regimes, such as along Côte D'Ivoire-Ghana ($\sim$700 km) or the Tasman Plateau ($>$600 km) (de Lépinay et al., 2016). Northwind Escarpment displays similarities in length and linearity with these other large continental margin strike-slip faults. The variability of the dip and morphology of the escarpment (Figure 5) suggests that local erosional and tectonic processes have modified it, similar to the transform segment of the Demerara Rise (Loncke et al., 2016). Lack of modern seismicity along the escarpment indicates it is not seismically active.

4.2. Chukchi Borderland

Northeast-trending features are evident in the bathymetric fabric (Figure 2a) within Chukchi Borderland (Brumley, 2009; Hall, 1990). The most prominent of these features is an elongate northeast-trending basin within Chukchi Plateau called the Egiazarov Trough (ET, Figures 1 and 2a), formerly called the Central Chukchi Basin by Brumley (2009) and Brumley et al. (2015). This trough is $\sim$175 km long by $\sim$30 km wide (i.e., an aspect ratio of almost 6:1), with vertical relief of more than 2,000 m. Slopes along the edges of the basin are commonly greater than 5° and locally more than 60° (Brumley, 2014). Although interpreted by Brumley (2009, 2014) to be caused by east-west extension, the Egiazarov Trough has limited seismic data that show faults with normal movement, steep, en-echelon faults of variable dips with little consistent thickening of the sedimentary section across the faults, and many horst blocks (Figure 6a). These geometries are similar to ones along similar sized pull-apart basins such as the Gulf of Aqaba at the south end of the Dead Sea (Ben-Avraham et al., 2008), where 6–8 km of sediment are contained within large normal faults on each side of the pull-apart basin and intrabasinal longitudinal and oblique faults form the internal structural fabric. The large aspect ratio of the Egiazarov Trough, its large depth, and complex faulting patterns could be alternatively interpreted as a pull-apart basin created by strike-slip transtensional faulting. Although pull-apart basins are often oblique to the bounding strike-slip faults, the orientation of the basins is dependent on many factors, including the stress field, the rheology of the heterogeneity of the basement, and thickness of the crustal brittle layer (e.g., Bertoluzza & Perotti, 1997; Gürbüz, 2010). Egiazarov Trough can be interpreted to be elongated parallel to the overall strike-slip motion, similar to other narrow basins in strike-slip zones (Smit et al., 2008). Other studies have shown that asymmetric half grabens can form along strike-slip faults without requiring extension (Katzman et al., 1995; ten Brink et al., 1996).

Without samples of the strata within the Egiazarov Trough, or interpretations of the seismic stratigraphy that tie or jump tie to seismic stratigraphy in Canada Basin, the age of this faulting remains speculative. However, the northeast strike of the trough is subparallel to the strike of Northwind Escarpment, indicating common structural orientation/basement control (e.g., Naylor et al., 1986) and likely kinematic history.

Other steep northeast-trending slopes exist in the borderland (Figure 2a), and a number of inferred northeast-trending faults have been mapped in the Geologic Map of North America (Garrity & Soller, 2009), indicating more widespread distribution of this fabric. On the western parts of the Chukchi Borderland, recent multichannel seismic reflection data show faulting of variable and opposing dip with local folding and inversion (Hegewald & Jokat, 2013; Ilhan & Coakley, 2016; Nikishin et al., 2014, 2017).

4.3. Sever Spur

Along northeastern Canada Basin, Sever Spur refers to the subparallel seafloor hills northwest of Prince Patrick Island that form the southeastern side of Stefansson Basin (Figures 1 and 2b). At least three prominent ridges within Sever Spur interrupt the otherwise smooth bathymetry of the margin (Figure 2b). These ridges are discontinuous segments up to ~100 km long, ~40 to 50 km apart, and 500–1,200 m high. While not as long as Northwind Escarpment, the northeastward trend of these ridges adds a location in the northern Canada Basin where a measureable northeast-trending fabric exists.

Multichannel seismic data collected across Sever Spur are similar to data from Northwind Escarpment, in that strata at the top of the ridges are truncated along steeply dipping surfaces interpreted as faults (Figure 6b). There is no evidence of folding or reverse offset that might indicate compressional deformation. Subparallel fault slivers are visible near km 49 (Figure 6b). Seismic reflection stratigraphic relations in the narrow basins between the ridges are more similar to symmetrical sag basins rather than asymmetric listric rift basins (km 50–65 and km 80–95, Figure 6b).

The faulted nature of the ridges, their higher elevation compared to the surrounding seafloor, and their position adjacent to the Canadian margin suggest that these features are part of extended continental crust. Helwig et al. (2011) include Sever Spur as part of the rifted North American margin in their schematic prerift reconstruction of Canada Basin. The Sever Spur ridges occur at the edge of the area mapped as HALIP (Figure 3a) (Oakey & Saltus, 2016; Saltus et al., 2011). Proximity of Sever Spur to the HALIP also complicates interpretations of stratigraphy and basement because of possible magmatic-related intrusion, extrusion, or deformation. On both the 4 and 150 km upward continued magnetic maps (Figures 3b and 3c), the Sever Spur ridges are at the junction of major changes in the magnetic field representing both shallow and deep crustal boundaries. These northeasterly trending bathymetric ridges, therefore, are similar to Northwind Escarpment and NoRMa, in that they fall along a first-order change in both shallow and deep magnetic properties and probably represent rifted continental crust adjacent to magmatic crust of the HALIP.

The evidence for strike slip or transtensional motion is indirect for the Sever Spur/HALIP boundary. The faults interpreted along the ridges of Sever Spur have normal offsets, demonstrated by their dip and geometry (Figure 6b), but the truncation of deposits atop the ridges is similar to the geometry of deposits truncated along the top of other strike-slip margins, such as Demerara Rise (Basile et al., 2013; Loncke et al., 2016) and the Amerasian side of Lomonosov Ridge, which is interpreted to be a trans-tensional margin (Cochran et al., 2006; Evangelatos & Mosher, 2016). The multiple ridges indicate that the structure is complex and possibly en-echelon. Like Northwind Escarpment, a plausible interpretation for both the sedimentary relations and geophysical anomalies is that Sever Spur is located along a transtensional crustal boundary at the edge of Canada Basin.

4.4. 78 N Basin

Multichannel seismic profiles show the presence of a large buried sedimentary basin near 78 N (Figure 6c). On the only near-orthogonal crossing of the basin, reflection data show that the basin is highly disrupted, with steep internal structures and abrupt changes in basement depth and dip (Figure 6c). Basin width is ~75 km and total sediment thickness within the synrift basin is ~3 km. Basement geometry does not resemble classic extensional half grabens with fan-shaped sedimentary reflections that formed along normal (listric) growth faults. Rather, the weak reflections in the synrift basin are discontinuous and dip in alternating directions. We call this basin the 78 N basin. The sonobuoy velocity data (Figure 6c) indicate that the

underlying crust is thinned continental in character and lacks the high-velocity lower crust interpreted further south as transitional crust (Chian et al., 2016).

While the large spacing between seismic lines precludes orienting the basin, an isolated rectangular-shaped negative gravity anomaly ~60 km wide by 175 km long coincides with the location of the 78 N basin (78 N, Figure 4a). The gravity anomaly is a negative anomaly of 20–40 mgal relative to the surrounding gravity field. On the seismic transect crossing the gravity low, the edges of the 78 N basin (Figure 6c) coincide with the edges of the gravity low (Chian et al., 2016), which suggests that the shape (rectangular) and orientation (northeast) of the gravity low are proxies for the shape and orientation of the basin.

Similarities between the general shape of the buried 78 N basin and the shape of the northern part of Chukchi Borderland suggest that the two features may have formed by similar processes at similar times, although Egiazarov Trough remains sediment starved (sedimentary fill <1 km with basement topography well preserved/imaged, Figure 6a) while the 78 N basin is infilled (more than 3 km of deposits within the synrift basin and an additional ~2 to 3 km covering the basement morphology making it difficult to image clearly, Figure 6c). The 78 N basin has many of the features of a pull-apart basin—rectangular in shape (gravity anomaly of Figure 4a) with multiple steep faults, horsts, and subbasins (Figure 6c), which are typical of pull-apart basins (Gürbüz, 2010; Mann, 2007). Fault dips generally range from 45° to 75°. Neither the seismic, magnetic, nor gravity data have sufficient resolution to further resolve details of the internal structure of the 78 N basin. Nor can we rule out that bright reflections from either the 78 N basin or from parts of Chukchi Borderland are caused by either sills or flows associated with the nearby HALIP, as suggested by Shimeld et al. (2016). The large distance of the 78 N basin from the shelf break of the Canadian margin attests to the complexity of the breakup and magmatic processes in this part of the polar margin.

The 78 N basin orientation is subparallel to and on strike with the trends of the Sever Spur ridges to the northeast (Figure 1). If these two features were once a tectonically continuous, they would form an elongate, stretched block of continental crust that is ~300 km long, as measured from the northernmost Sever Spur ridge to the south end of the 78 N basin. The coincidence of the northern edge of the rectangular gravity anomaly of the 78 N basin with a bend in the edge of the HALIP (Figure 4a) suggests that the 78 N basin may have somehow acted as a barrier to HALIP.

4.5. Alaska-Prince Patrick Magnetic Lineament—APPL

A narrow, northeast-trending, linear negative magnetic lineament exists in southeastern Canada Basin (Figure 3a), herein called the Alaska Prince Patrick magnetic Lineament or APPL. The lineament is a narrow (<30 km wide) magnetic low of 50–60 nT amplitude that can be traced from offshore Prince Patrick Island to near the bend in the Canada Basin Gravity Low (CBGL), for a distance of 600 km (Figure 3a). APPL truncates the magnetic anomalies along the southeastern edge of the polygon of oceanic crust, contributing to a visual impression that the oceanic magnetic anomalies are fan shaped (e.g., Embry, 1990; Grantz et al., 1990b, 1998, 2011; Taylor et al.,1981). APPL continues an additional 500 km toward the Alaskan continental margin less distinctly as a set of discontinuous magnetic lows along the southeastern boundary of the D3′ domain. Although a small anomaly, APPL is visible in the 4 km upward continued magnetic data as a magnetic trough within a generally subdued magnetic field of Canada Basin (Figure 3b). Both the APPL and its discontinuous extension are more than 1,100 km long, from onshore Alaska to the continental margin of Canada offshore Prince Patrick Island.

APPL may also have a deep-seated expression. In the first vertical derivative of the 150 km upward continued data (Figure 3c), APPL separates broad, oblong negative anomalies on the southeast from an elongated positive anomaly, D3′, on the northwest. The crustal velocities from Chian et al. (2016) indicate that this part of APPL separates a block of high-velocity transitional crust/serpentinized mantle on the southeast from a block of lower velocity continental crust to the northwest (D3′). Likewise, APPL crosses the southeastern corner of the polygon of oceanic crust (Figure 3a). The association of APPL with the boundaries of oceanic, transitional, or continental crust suggests it either controlled or contributed to the formation of these crustal boundaries, and, because of that role, may predate or be synchronous with the formation of the basin.

The basement beneath APPL is not imaged in the multichannel data because basement is deeper than and obscured by the first multiple reflection. In this part of Canada Basin, basement is more than 12 km deep beneath the thick sediment wedge of the Mackenzie Fan (Grantz et al., 1990b; Shimeld et al., 2016). The

APPL lineament does not have an equivalent lineation or anomaly in gravity or upward continued gravity maps (Figure 4), suggesting it does not represent a significant density boundary. Gravity anomalies along the boundaries between transitional and oceanic crust of the hyperextended Iberian margin are also small, ~10 mgal, (Dean et al., 2000) and essentially indiscernible (Catalao, 2006) suggesting that a gravity anomaly is not a required condition at these kinds of crustal changes. APPL does, however, project into the Canadian margin offshore of Prince Patrick Island where the gravity data show a major saddle and change in direction of the shelf-edge paired positive-negative anomaly (SEPA of Figure 4a). This paired anomaly is a first-order anomaly that dominates the gravity field along continental margins and represents the gravitational effects of changes in water depth, sediment thickness, and crust/mantle depth (Vogt et al., 1998). The intersection of APPL with SEPA marks a fundamental change in the geometry and direction of the Canadian continental margin near Prince Patrick Island.

5. Discussion

5.1. Northeast Trends and Crustal Structure

Northwind Escarpment on the west side of Canada Basin is the most prominent northeast-trending feature in Canada Basin. Our interpretation that the escarpment is part of major strike-slip crustal boundary is consistent with earlier observations that it is a transform fault located along a small circle from a pole of rotation in the Mackenzie River delta region (Funck et al., 2011; Grantz et al., 1979; Shipilov & Lobkovskii, 2014; Vogt et al., 1982). Other authors have proposed models in which a major strike-slip crustal boundary extends from the Chukchi Shelf northward along either Northwind Escarpment (Freeland & Dietz, 1973; Nikishin et al., 2014) or within the Chukchi Borderland (Chekhovich et al., 2015).

Geologic and geophysical evidence support the interpretation that northeast-trending structures within the Chukchi Borderland are essentially continuous with similar structures on the Chukchi Shelf. Seismic observations from the Chukchi Sea shelf and southern Chukchi Borderland, and descriptions and quantitative geochronology and thermochronology of dredge samples from the northern Chukchi Borderland demonstrate fundamental differences in pre-Mississippian basement rocks between the Chukchi Platform and Plateau on the west and the Hanna Trough, Northwind Basin, and Northwind Ridge on the east (Connors & Houseknecht, 2017; Ilhan & Coakley, 2016; Kumar et al., 2011; Miller et al., 2017; O'Brien et al., 2016; Sherwood, 1994; Sherwood et al., 2002). Beneath the Chukchi Shelf, a crustal boundary is marked by a major change in reflectivity from transparent crust on the west to highly reflective crust on the east beneath Hanna Trough (Kumar et al., 2011). Results of previous coring and recently collected seismic data indicate the presence of Ellesmerian strata beneath the Northwind Basin and Ridge, and these likely correlate with the sedimentary fill of the Hanna Trough (Grantz et al., 1998; Ilhan & Coakley, 2016; Kumar et al., 2011; Sherwood et al., 2002). All these observations suggest that the Hanna Trough and Northwind Basin and Ridge, now separated by the narrow (100 km) eastern end of the North Chukchi Basin, were originally a single extensional basin that developed above a tectonic feature that has been interpreted as a Caledonian suture between Timanian and Laurentian crust (Miller et al., 2017; O'Brien et al., 2016). Thus, the boundaries between the Chukchi Platform and Hanna Trough on the Chukchi Shelf (yellow-gray dashed line, Figure 1) and between the Chukchi Plateau and Northwind Basin on the Chukchi Borderland (yellow-gray dashed lines, Figure 1) represent approximate tectonic lines of reference for considering the relative positions of Arctic Alaska and the Borderland following the Caledonian orogeny. These lines display no significant difference in orientation, implying little or no rotation of the Chukchi Borderland relative to the Chukchi Shelf. The lines on the Chukchi Borderland do, however, appear to be offset by a modest distance (<50 km) to the east. The cause of this eastward translation is unknown, although it may be related to post Ellesmerian extension that has been proposed by numerous authors (e.g., Grantz et al., 1998).

At ~300 km long, the combined Sever Spur/HALIP and 78 N basin boundary in the northern Canada Basin (yellow-gray dashed line, Figure 1—Sever Spur) forms the second major northeast-trending feature. The boundary is approximately half the length of the 600 km long Northwind Escarpment and has much lower morphologic expression in the three Sever Spur ridges. This feature marks the fundamental change in magnetic character from the high amplitudes of the HALIP to more subdued amplitudes along the continental margin and has both shallow and deep magnetic and gravity signatures (Figures 3 and 4). This boundary separates inferred extended continental crust of Sever Spur from the highly mafic crust of HALIP.

Interestingly, if the 78 N basin and the ridges of Sever Spur are part of a single subsided, extended block of continental crust, they are approximately on trend with the D3′ block that extends north from Alaska (Figure 3a, CC in Figure 1). Both the D3′ block and the 78 N basin are interpreted as extended continental crust that are located unusually outboard into Canada Basin (>250 km) and must be accounted for in reconstructions of Canada Basin.

A third large northeast-trending feature within the Canada Basin is APPL. Although the narrow width and small amplitude of the APPL magnetic lineament implies it comes from a shallow source, the 150 km upward continued magnetic data (Figure 3c) suggest it may also coincidentally mark the edge between a deeper nonmagnetic (or very low magnetic domain) to the southeast and somewhat more magnetized material to the northwest in Canada Basin. APPL occurs along the southeastern boundary of oceanic crust (Chian et al., 2016), although sonobuoy control is sparse in this region.

Each of these three features—Northwind Escarpment, the Sever Spur/78 N boundary, and APPL—coincides with an observed or inferred change in crustal type. Any interpretation of the tectonic evolution and opening of the Canada Basin needs to account for these crustal changes and their orientations.

The structure of the Amerasia Basin north of Canada Basin is masked by the high magnetic and gravity anomaly values associated with the HALIP. Makarov Basin, within the HALIP between Alpha and Lomonosov Ridges, may provide a window into this underlying structure. While a portion of the basin is underlain by HALIP volcanics, a segment adjacent to Lomonosov Ridge exhibits possible oceanic crustal velocities (Evangelatos & Mosher, 2016; Evangelatos et al., 2017). The Amerasia side of Lomonosov Ridge has been interpreted as a transform margin (Cochran et al., 2006), and a transform may occur beneath the Alpha and Mendeleev Ridges (the Amerasian Basin Transform of Doré et al., 2016). The Makarov Basin is interpreted as a transtensional basin, (Evangelatos et al., 2017). If these interpretations are correct, they are part of a pattern of transtentional tectonics that formed the entire Amerasia Basin, as suggested by Doré et al. (2016).

5.2. Age of Northeast-Trending Features

In our interpretation, the Northwind Escarpment and the Sever Spur/78 N boundaries separate major crustal types within Canada Basin that are associated with the initial formation of Canada Basin. They are therefore at least as old as the Cretaceous age of opening (Chian et al., 2016; Embry & Dixon, 1994). Without ages or dated samples of the deepest sediments, it is impossible to constrain the age of faulting that offsets basement and shallower sediments. Initial lithologic comparisons of basement rocks cored from Northwind Escarpment correlate them with similar rocks mapped on the Canadian Arctic Islands (Grantz et al., 1998). Dating of basement rocks dredged from Northwind Escarpment correlates them with Cambrian platform rocks of the Paleozoic continental margin that crops out on Ellesmere Island in Canada (O'Brien et al., 2016) and is known in boreholes on the Chukchi Shelf (Hubbard et al., 1987; Kumar et al., 2011; Sherwood et al., 2002), suggesting Chukchi Borderland was once continuous with these two continental margins now separated by ~2,000 km. Whether these older Paleozoic structures formed preexisting zones of weakness during the breakup process that formed Canada Basin remains speculative. The age of APPL is not possible to determine since it is only identified in the magnetic data as a lineament. Its location mostly outside of the polygon of oceanic crust may indicate it is older than the oceanic crust.

5.3. Two-Phase Model to Explain the Northeast-Trending Features

Using these northeast-trending features (Northwind Escarpment, Sever Spur/78 N basin, and APPL) and the crustal types presented in Chian et al. (2016), we present a conceptual model for the opening of Canada Basin (Figure 7). This model therefore incorporates constraints from the new seismic data from the Canada Basin that were not available in previous models. Both strike-slip and rotational movements are used in our model. Figure 7 shows four snap shots of basin evolution: (a) closure; (b) phase 1 rifting/transtension; (c) phase 2 seafloor spreading; and (c) current configuration.

Closure shows Arctic Alaska and the Chukchi Borderland positioned adjacent to the Canadian Arctic Islands (brown polygons, Figure 7a). Three aspects of the Chukchi Borderland are (a) it has been reduced in east-west width (current coordinates) to close Northwind Basin, i.e., the basin between Northwind Ridge and the Chukchi Plateau, similar to the closures presented by Shephard et al. (2013), Amato et al. (2015), and O'Brien et al. (2016); (b) it is not significantly rotated relative to Arctic Alaska, i.e., closure is only to the point where the Chukchi Borderland obliquely touches the Canadian margin near Ellesmere Island; and (c) the North

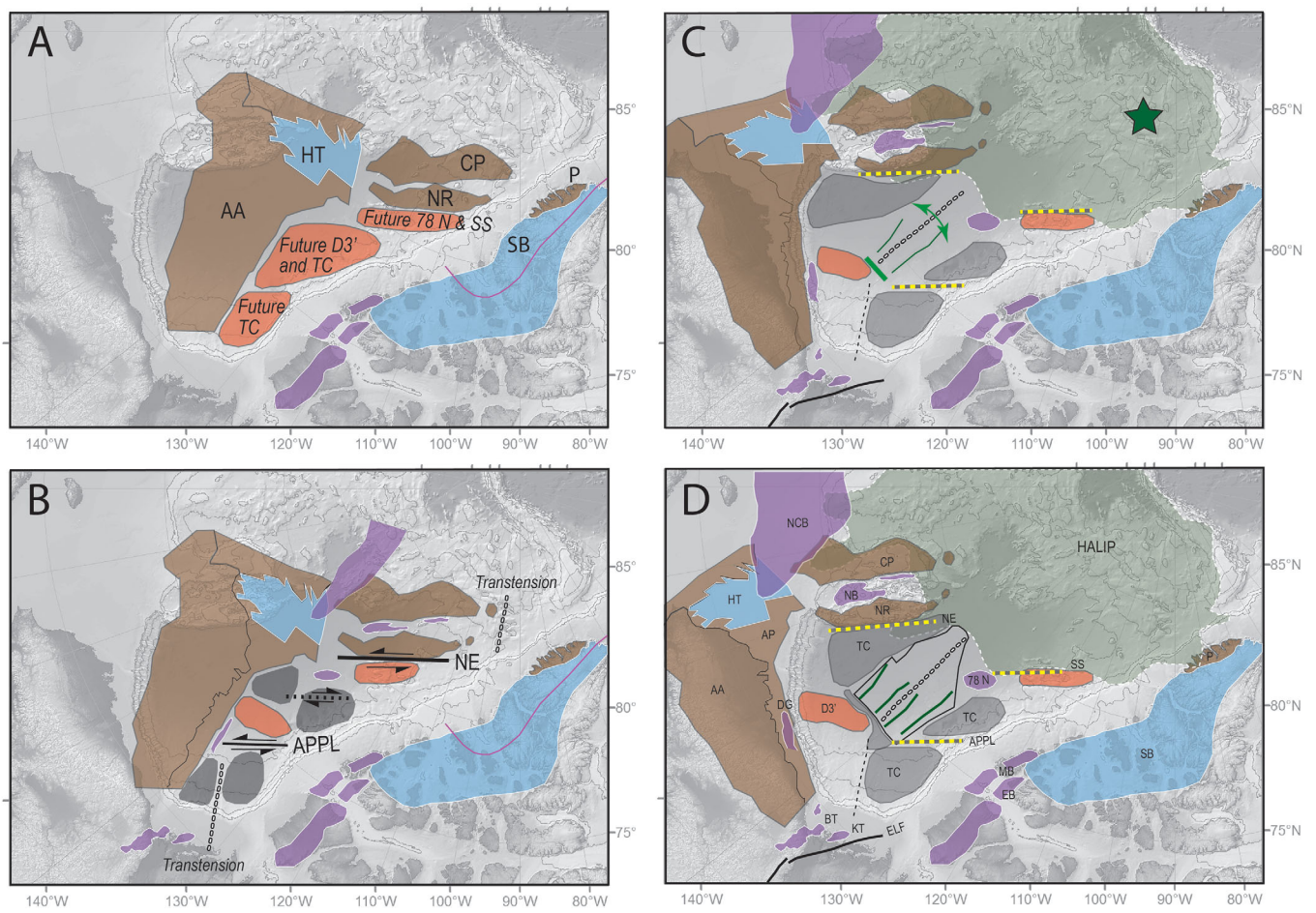

Figure 7. Conceptual model for the evolution of the Canada Basin. Abbreviations are the same as Figure 1, adding AA, Arctic Alaska; AP, Arctic Platform; CP, Chukchi Plateau; P, Pearya; SS, Sever Spur; NR, Northwind Ridge. (a) Closure. (b) Phase 1 rifting showing strike-slip extension and transtension. (c) Phase 2 seafloor spreading showing rotation. (d) Present time. See text for additional explanation.

Chukchi Basin is closed (NCB, Figures 1 and 7d), reducing the distance between the Hanna Trough and Chukchi Borderland. The position of the Borderland near the Canadian coast is similar to that determined by lithologic, zircon, and age dating analyses from dredge samples that correlate the Chukchi Plateau with the Pearya terrane on Ellesmere Island and Northwind Ridge with Laurentian (Cambrian Franklinian) rocks to the south of Pearya (P in Figure 7d) (Knudsen et al., 2017; O'Brien et al., 2016). Our position of the Chukchi Borderland is slightly to the north of that proposed by O'Brien et al. (2016) and Grantz et al. (1998), so that the Chukchi Borderland is adjacent to and does not overlap Sever Spur.

As discussed in section 5.1, Chukchi Borderland is not significantly rotated relative to Arctic Alaska since the Paleozoic Caledonian Orogeny. A consequence of maintaining the current geometry between the Chukchi Borderland and Arctic Alaska is that Alaska does not close completely against the Canadian Arctic Islands. Our model fills this space with continental blocks that will stretch to become the large blocks either of extended continental crust trapped and subsided within the basin (Sever Spur, 78 N, and D3' blocks) or of high-velocity transitional crust mapped by Chian et al. (2016) that surround mapped oceanic crust (blocks labeled future TC in Figure 7a). While we have little information on the geometry, morphology, or lithology of these blocks, they might be the offshore continuation of the inverted Ellesmerian foreland basin strata that provided the source of sedimentation in northern Alaska between Pennsylvanian and Middle Jurassic time (Gottlieb et al., 2014).

During phase 1 rifting/transtension (Figure 7b), extension would have been subparallel to the northeast orientations of Northwind Escarpment, the ridges of Sever Spur, and APPL. Depending on location within

these blocks, rift basins formed either with a pull-apart geometry (such as the basins in the Chukchi Borderland) or as half-graben or full graben geometries (such as Dinkum Graben and the North Chukchi Basin). The North Chukchi Basin, oriented perpendicular to the inferred direction of extension, is the largest and deepest of the synrift basins that formed at this time, and its opening may have contributed to a small relative rotation or offset between the Chukchi Borderland and the Chukchi Shelf. Most of the Canadian Arctic coast is oblique to the inferred direction of extension, which may explain why synrift basins on, for example, Prince Patrick Island are not well-defined half graben (Harrison & Brent, 2005). During this rifting stage, the blocks of continental crust between Arctic Alaska and the Canadian Arctic Islands (shown in Figure 7a) are stretched and begin to be identified as the thinned continental (orange) or transitional (gray) crustal blocks that will surround future oceanic crust of the Canada Basin.

Although not constrained by our data, additional strike-slip faults probably occur during this rifting event, for example, along the eastern edge of the Chukchi Plateau associated with formation of Northwind Basin and Egiazarov Trough. The eastern edge of the Chukchi Plateau is interpreted as a Paleozoic terrane boundary (O'Brien et al., 2016), and therefore could be a preexisting crustal weakness reactivated during rifting. A speculative dextral strike-slip fault is shown in the center of the basin (dashed line in Figure 7b), or, possibly, the entire area of the center of the Canada Basin was a zone of extension or transtension between two areas of potential orthogonal extension (white dotted lines in Figure 7b). APPL, possibly defining a southern boundary to the zone of transtension may be a continuation of the rift transfer zone faults proposed at the south end of the Sverdrup Basin (Hadlari et al., 2014). The Cretaceous (ancestral) phase of Brooks Range orogeny would have been fully developed during this rift stage as the Angayucham Ocean south of Alaska (current coordinates) closed (e.g., Moore et al., 1994; Moore & Box, 2016, and references therein).

Phase 2 initiates seafloor spreading. Figure 7c shows the Canada Basin after the formation of the first set of magnetic anomalies (green lines). A change in spreading direction has occurred so that opening is about a speculative pole to the south, i.e., along the extension of the northern axis of the CBGL, rather than along the CBGL that projects into the Mackenzie River region, as proposed by other authors (Embry, 1990; Grantz et al., 1990b, 1998, 2011; Lawver et al., 2002; Shephard et al., 2013; Taylor et al., 1981). This pole was determined so as (a) to place a possible transform/fracture zone at the very narrow transition from continental block D3′ to oceanic crust constrained by refraction results (Chian et al., 2016) (heavy green line, Figure 7c), and (b) to be oriented along strike of inferred oceanic magnetic anomalies (Figure 3a). In our model, APPL truncates the magnetic anomalies within the eastern half of the polygon of oceanic crust. APPL contributes to a visual impression that the oceanic magnetic anomalies are fan shaped (e.g., Embry, 1990; Grantz et al., 1990b, 1998, 2011; Taylor et al., 1981). Original rotational opening was estimated at 66° using onshore paleomagnetics (Halgedahl & Jarrard, 1987), and at 55° using a modified closure configuration (Gottlieb et al., 2014), but rotation fails to explain the asymmetry of oceanic crust in the Canada Basin based on refraction results (Chian et al., 2016). While the rotation model still best explains geological links between Alaska and the Canadian Arctic, rotation may be less than these previous models use.

The spreading center is shown by the white dotted line and its possible oblique continuation toward the Mackenzie River delta (light black dashed line). Because extension on the continuation toward the Mackenzie River delta would have been oblique, this geometry may explain why transitional crust (serpentinized mantle) is found in this region, similar to the oblique spreading in the Knipovich Ridge in the eastern Arctic (Jokat et al., 2012; Kandilarov et al., 2010). The North Chukchi Basin has opened by this time, yielding the final relative positions between the Chukchi Borderland and the Chukchi Shelf/Hanna Trough.

The earliest volcanism of HALIP at ~130 Ma (Evenchick et al., 2015) is inferred to overlap in time with the seafloor spreading of the Canada Basin (Chian et al., 2016), so that the continuation of the seafloor spreading axis to the north has been obscured. The location of a eruption center associated with the HALIP (Døssing et al., 2013) is shown by the green star (Figure 7c). During the change in spreading direction, the Northwind Escarpment fault may have acted as a leaky transform allowing magmatism from HALIP to intrude southward along the fault as the source of the NoRMA anomaly. The Sever Spur and APPL structures may also have undergone oblique transtension during the change from rifting to seafloor spreading.

5.4. Implications of the Two-Phase Model

Our two-phase opening of the Canada Basin differs from the currently accepted rotational model (Grantz et al., 2011) in several respects. First, the rifting phase in our model is dominated by strike-slip motions that

explain the orientations and locations of Northwind Escarpment, Sever Spur, the buried 78 N basin and APPL. This differs from the Grantz et al. (2011) model in which rifting is rotational with a strike-slip boundary along Lomonosov Ridge. Second, our model more evenly divides the amount of opening between rifting and seafloor spreading, rather than having wider separation during rifting than during seafloor spreading as in the Grantz et al. (2011) model. Third, our model involves a change in orientation of extension between rifting and seafloor spreading, in contrast to the Grantz et al. (2011) model which has rotational extension during both phases. Changes between the direction of extension during rifting and seafloor spreading are known, with a good example from the Gulf of Mexico, where regional northwest-southeast extension during rifting changed to rotational opening by seafloor spreading around a pole located in western Cuba (Nguyen & Mann, 2016). This change from transtension to extension has also been proposed for the opening of the Amerasian Basin at its northern limits along Lomonosov Ridge (Evangelatos & Mosher, 2016).

Doré et al. (2016) propose a model for the opening of the Canada Basin in which rotation is accompanied by a transform fault that underlies the Alpha and Mendeleev Ridges. While there are few data to constrain the location of their proposed transform fault, our model uses data from Northwind Escarpment to suggest its 600 km length, linear morphology, accompanying abrupt crustal changes, and seismic stratigraphic relations make it a better candidate for a transform boundary. Rather than a 45 million years duration of seafloor spreading (125–80 Ma) that creates oceanic crust across the entire width of the Canada Basin (Doré et al., 2016), our model has a much shorter duration ($<$10 Ma) prior to the onset of the Cretaceous positive polarity chron at 124 Ma in which oceanic crust is created in the center of the basin where constrained by sonobuoy data, as proposed by Chian et al. (2016).

Our model allows the Chukchi Borderland to be a microcontinental block essentially fixed with respect to Arctic Alaska prior to rifting, which most other models of the opening have not been able to accommodate (Amato et al., 2015; Doré et al., 2016; Grantz et al., 1990b; Lawver et al., 2002; Miller et al., 2010; Shephard et al., 2013). Development of the Chukchi Borderland in a strike slip or transtensional environment is consistent with recent reviews of the formation of microcontinents (Nemčok et al., 2016) and marginal plateaus along continental margins (de Lépinay et al., 2016) which overwhelmingly evolve in sheared settings. The placement of the Chukchi Borderland as a coherent block outboard of Ellesmere Island provides supporting evidence for it to be part of Crockerland, the missing northern source area for sediments along the Canadian polar margin during Triassic to Middle Jurassic times (Embry, 2009), also hypothesized by various authors (e.g., Brumley et al., 2015; Drachev, 2016; O'Brien et al., 2016). Our model explains the distribution of crustal types identified in the Canada Basin from refraction data (Chian et al., 2016). While these refraction data are new, they provide important constraints that were not previously available.

Finally, although our model is that the Chukchi Borderland developed in a strike-slip/transtensional rifting regime, the Borderland could also be modeled as a strike-slip transform margin. In addition to the length and linearity of transform margins, many are characterized by marginal plateaus, a marginal ridge, steep slopes conducive to gravity-driven collapse, regional erosional unconformities, and a narrow continent-ocean transition (de Lépinay et al., 2016). These characteristics are present for the Borderland (Chukchi Plateau, Northwind Ridge, submarine landslides (Brumley, 2014), regional unconformities (Arrigoni, 2008; Hegewald & Jokat, 2013), and a narrow continent-ocean transition (Chian et al., 2016; Hall, 1990). At $\sim$600 km long, the length of Northwind Escarpment is similar to lengths of transform margins such as the Tasman Plateau or Cote d'Ivoire-Ghana margin, but less than, for example, the Falklands-Malvinas margin (de Lépinay et al., 2016). If Northwind Escarpment evolved as a transform margin, one implication is that it would have been associated with an earlier, older phase of seafloor spreading, creating oceanic crust around the edges of Canada Basin. Refraction results of Chian et al. (2016) show that transitional crust rather than oceanic crust is immediately adjacent to Northwind Ridge, so this transform interpretation is less likely.

5.5. Future Directions

Although our model can explain new observations and propose alternatives explanations for locations of features such as Chukchi Borderland, it also raises new questions and new hypotheses to test. Our model is conceptual in nature and needs to be tested by numerical models accounting for constraints from global plate reconstructions for Siberia, North America, and Europe, similar to those carried out in the past (Amato et al., 2015; Doré et al., 2016; Lawver et al., 2002; Shephard et al., 2013). Particularly important will be testing how reasonable it is for Alaska to be distant from, although continuous with the Canadian Arctic as shown

in our model. Part of testing our model will be determining the geometry of synrift basins within Chukchi Borderland and how they constrain its early evolution (e.g., Ilhan & Coakley, 2016).

While our model utilizes rotation during seafloor spreading, the magnetic anomalies are actually more subparallel in their geometry than fanning (Figures 3 and 7), which was the original rationale for rotation (e.g., Grantz et al., 1990b; Vogt et al., 1982). Hence, the requirement for a nearby pole is not necessarily warranted. Likewise, the shape of the polygon of oceanic crust suggests that the pole could be northward, in the direction of narrowing of the polygon of oceanic crust. The overprinting of this northern region by HALIP volcanism (Oakey & Saltus, 2016; Saltus et al., 2011), the triangular shape of Canada Basin, and the compelling geologic evidence linking Arctic Alaska to Canada (Gottlieb et al., 2014; Mickey et al., 2002) makes this pole-to-the-north possibility difficult to accept.

A further idea to pursue is whether the seafloor spreading direction could be oblique, similar to the disrupted anomalies in the Lena Trough or Knipovich Ridge, which currently have highly oblique opening directions within the North Atlantic/Arctic spreading center in the eastern Arctic (e.g., Engen et al., 2008). The magnetic anomalies in Canada Basin are short segments of discontinuous ovoid anomalies (Figure 3) that have not been easy to identify and date (Chian et al., 2016; Coles & Taylor, 1990; Grantz et al., 2011; Taylor et al., 1981; Vogt et al., 1982). While some of this may be due to the 4–6 km thick sediments overlying the basement (Grantz et al., 1990b; Shimeld et al., 2016), an alternative explanation is that the discontinuous anomalies are the result of oblique spreading. In the recent analysis of Chian et al., (2016), a conundrum exists in fitting the magnetic anomalies—either the rate of opening is too fast to explain the observed rugged seafloor topography, which implies ultraslow spreading (e.g., Ehlers & Jokat, 2009), or the ages of the magnetic anomalies cannot be reasonably accurately fit.

The magnetic APPL merges with the southern boundary of the D3′ block of continental crust north of Alaska (Figure 1) and is proximal to the bend north-northeastward of the active deformation front of the Brooks Range (Active Frontal Thrust of Figure 1). Our data raise the possibility that the sharp northward bend in the Brooks Range deformation may in fact be controlled by the D3′/APPL boundary. The magnetic character of domains similar to D3 has been interpreted to be part of rheologically stiff crustal components that could form buttresses to deformation (Hyndman et al., 2005; Saltus & Hudson, 2007), suggesting a cause for the northeast deflection of Brooks Range deformation into the Canada Basin. While this cause and effect scenario is speculative, it suggests APPL could be reflecting both ancient rifting and modern tectonic processes, also a topic for future research.

6. Summary

Analysis and integration of multiple geological and geophysical data sets reveals the existence of three subparallel, north-east-trending structures in Canada Basin of the Arctic Ocean that are interpreted as evidence of strike slip, or transtensional tectonic deformation in the early formation of Canada Basin. These features are:

1. Northwind Escarpment, more than 600 km long and up to 2,800 m relief. This escarpment is a crustal boundary separating extended continental crust beneath Northwind Ridge/Chukchi Borderland from thinner transitional (intruded?) crust in the adjacent Canada Basin. Seismic stratigraphic relations do not support pure extensional or compressional deformation along the escarpment and our preferred interpretation is that it represents a large strike-slip fault that is at least as old as Canada Basin, although it, and subparallel trends on the Chukchi Borderland may have been influenced younger Paleogene postrift deformation. The NoRMA magnetic anomaly just east of Northwind Escarpment may be evidence for a leaky transform from the HALIP.
2. The Sever Spur/78 N feature is smaller, about half the length of Northwind Escarpment with lower relief along the subparallel Sever Spur ridges. Like Northwind Escarpment, it is a crustal boundary inferred to separate continental crust of Sever Spur from magmatic crust of the HALIP. Strike slip or transtensional motion is based on the projection of the Sever Spur/HALIP boundary to the 78 N basin that is interpreted as a pull-apart based on steep faults with opposing dips, horst blocks and variably rotated fault blocks. Direction of motion along the Sever Spur/78 N feature is not resolved with current data.
3. The APPL lineament, based on magnetics, is least well resolved. APPL truncates magnetic anomalies of oceanic crust along the southeastern edge of the polygon of oceanic crust. APPL projects northeastward

to a major saddle or break in the shelf-edge paired gravity anomaly where the Canadian polar margin changes orientation from north to northeast. APPL projects southwestward along the boundary separating continental of the D3′ magnetic domain from transitional crust of the Beaufort-Mackenzie region. APPL is roughly on strike with the northward bend in the active deformation front of the Brooks Range.

A conceptual model to account for these features involves a two-phase opening of the Canada Basin. In closure, the Chukchi Borderland is not rotated relative to Arctic Alaska, but rather is restored to a position near Pearya on northern Ellesmere Island similar to the reconstruction by (O'Brien et al., 2016), placing it in a position where it could be part of the missing Crockerland of Embry (2009). In this closure, a gap exists between Arctic Alaska and the Canadian Arctic which we speculate might have been occupied by the D3′ and 78 N continental crustal blocks now subsided beneath the Canada Basin, as well as transitional crust now surrounding oceanic crust, as mapped by Chian et al. (2016).

In the first phase of opening, rifting proceeded with strike slip or transtensional motion along the three northeast-trending features and the development of pull-apart basins on the Chukchi Borderland and in the 78 N basin. Some differential motion between the Chukchi Shelf and Chukchi Borderland may have been accommodated with the formation of the North Chukchi Basin. In the second phase, rotational opening completed the formation of oceanic crust and the configuration of crustal blocks as we know them today. This model raises many new questions and avenues of research to test its implications and accuracy.

Acknowledgments

This paper grew out of discussions during writing the "Distribution of Crustal Types in Canada Basin, Arctic Ocean" by Chian et al. (2016), and raised questions that were too many to include in that paper. We have benefitted from many discussions and challenges from Larry Lane and colleagues too numerous to name individually, and we are grateful that they engaged us and improved our final product. The multichannel seismic data used in this paper were enabled by the officers and crews of the CCGS *Louis S. St-Laurent* and the USCGC *Healy*. We were also dependent on the experience, skill and dedication of the seagoing technical team lead by Borden Chapman. Daniel Scheirer provided excellent feedback through review of an early version of the manuscript. Reviews by S. Drachev, U. ten Brink, Patrick Potter, and an anonymous reviewer are appreciated and helped clarify our results. Funding for this work was provided in part through the Geological Survey of Canada as part of Canada's UNCLOS Project and through the U.S. Geological Survey as part of the U.S. Extended Continental Shelf project. The findings and conclusions stated herein are those of the authors and the U.S. Geological Survey but do not necessarily reflect the views of other U.S. Continental Shelf agencies or the Canadian UNCLOS project. This is Earth Science Sector (Canada) ESS contribution no. 20170270. The digital multichannel seismic reflection data used in Figures 5 and 6 of this paper are available in Mosher et al. (2016) at (http://geoscan.nrcan.gc.ca/). The digital multichannel seismic reflection data from Figure 6a are available through Shipley et al. (2012) at http://www-udc.ig.utexas.edu/sdc/cruise.php?cruiseIn=hly0503. All other bathymetric and potential field data used in this paper are available through publications cited in the text.

References

Amato, J. M., Toro, J., Akinin, V. V., Hampton, B. A., Salnikov, A. S., & Tuchkova, M. I. (2015). Tectonic evolution of the Mesozoic South Anyui suture zone, eastern Russia: A critical component of paleogrographic reconstructions of the Arctic region. *Geosphere*, *11*(5), 1530–1564. https://doi.org/10.1130/GES01165.1

Andronikov, A., Mukasa, S., Mayer, L. A., & Brumley, K. (2008). First recovery of submarine basalts from the Chukchi Borderland and Alpha/Mendeleev Ridge, Arctic Ocean. Abstract #V41D-2124 presented at Fall Meeting 2008, American Geophysical Union, Washington, DC.

Arrigoni, V. (2008). *Origin and evolution of the Chukchi Borderland* (MSc thesis, 74 pp.). College Station, TX: Texas A&M University.

Basile, C., Maillard, A., Patriat, M., Gaullier, V., Loncke, L., Roest, W., . . . Pattier, F. (2013). Structure and evolution of the Demerara Plateau, offshore French Guiana: Rifting, tectonic inversion and post-rift tilting at transform-divergent margins intersection. *Tectonophysics*, *591*, 16–29. https://doi.org/10.1016/j.tecto.2012.01.010

Ben-Avraham, Z., Garfunkel, Z., & Lazar, M. (2008). Geology and evolution of the southern Dead Sea Fault with emphasis on subsurface structure. *Annual Review of Earth and Planetary Sciences*, *36*, 357–387. https://doi.org/10.1146/annurev.earth.36.031207.124201

Bertoluzza, L., & Perotti, C. R. (1997). A finite-element model of the stress field in strike-slip basins: Implications for the Permian tectonics of the Southern Alps (Italy). *Tectonophysics*, *280*(1–2), 185–197.

Blakely, J. R. (1996). *Potential theory in gravity and magnetic applications* (441 pp.). Cambridge, UK: Cambridge University Press.

Brumley, K. (2009). *Tectonic geomorphology of the Chukchi Borderland: Constraints for tectonic reconstruction models* (M.Sc. thesis, 116 pp.). Fairbanks: University of Alaska.

Brumley, K. (2014). *Geologic history of the Chukchi Borderland, Arctic Ocean* (PhD dissertation, 253 pp.). Stanford, CA: Stanford University. Retrieved from https://purl.stanford.edu/hz857zk1405

Brumley, K., Miller, E. L., Konstantinou, A., Grove, M., Meisling, K. E., & Mayer, L. A. (2015). First bedrock samples dredged from submarine outcrops in the Chukchi Borderland, Arctic Ocean. *Geosphere*, *11* (2), 76–92. https://doi.org/10.1130/GES01044.1

Carey, S. W. (1955). The orocline concept in geotectonics. *Proceedings of the Royal Society of Tasmania*, *89*, 255–288.

Catalao, J. (2006). Iberia-Azores Gravity Model (IAGRM) using multi-source gravity data. *Earth Planets Space*, *58*, 277–286.

Chekhovich, V. D., Lobkovskii, L. I., Kononov, M. V., & Sheremet, O. G. (2015). Late Cretaceous-Paleogene transform zone between Eurasian and North American lithospheric plates. *Geotectonics*, *49*(5), 361–378.

Chian, D., Jackson, H. R., Hutchinson, D. R., Shimeld, J. W., Oakey, G. N., Lebedeva-Ivanova, N., . . . Mosher, D. C. (2016). Distribution of crustal types in Canada Basin, Arctic Ocean. *Tectonophysics*, *691*, 8–30.

Chian, D., & Lebedeva-Ivanova, N. (2015). *Atlas of sonobuoy velocity analyses in Canada Basin* (Geological Survey of Canada Open File 7661, 55 pp.). Retrieved from http://ftp2.cits.rncan.gc.ca/pub/geott/ess_pubs/295/295857/of_7661.zip

Churkin, M., Jr., & Trexler, J. H., Jr. (1980). Circum-Arctic plate accretion—Isolating part of a Pacific plate to form the nucleus of the Arctic Basin. *Earth and Planetary Science Letters*, *48*(2), 356–362.

Coakley, B., Kristoffersen, Y., & Hopper, J. (2005). *Cruise report for underway geophysics program HLY 05-03, 5 August 2005; Dutch Harbor, Alaska to 30 September, 2005; Tromso, Norway* (84 pp.). Retrieved from http://www-udc.ig.utexas.edu/sdc/functions/download.php?file=/DBother/hly0503/hly0503.mgg.cruiserpt.pdf

Cochran, J. R., Edwards, M. H., & Coakley, B. J. (2006). Morphology and structure of the Lomonosov Ridge, Arctic Ocean. *Geochemistry, Geophysics, Geosystems*, *7*, Q05019. https://doi.org/10.1029/2005GC001114

Coles, R. L., & Taylor, P. (1990). Magnetic anomalies. In A. Grantz, K. Johnson, & J. F. Sweeney (Eds.), *The Arctic Ocean region* (pp. 119–132). Boulder, CO: Geological Society of America, Geology of North America.

Connors, C. D., & Houseknecht, D. W. (2017). Hanna and her sisters—Structural inheritance in the Chukchi Sea, Alaska [Abstract]. *American Association of Petroleum Geologists Pacific Section*, 25–26.

Dean, S. M., Minshull, T. A., Whitmarsh, R. B., & Louden, K. E. (2000). Deep structure of the ocean-continent transition in southern Iberai Abyssal Plain from seismic refraction profiles: The IAM-9 transect at 40°20′N. *Journal of Geophysical Research*, *105*, 5859–5885.

de Lépinay, M. M., Loncke, L., Basile, C., Roeset, W. R., Patriat, M., Mailard, A., & De Clarens, P. (2016). Transform continental margins—Part 2: A worldwide review. *Tectonophysics*, *693*, 96–115.

Dick, H. J. B., Lin, J., & Schouten, H. (2003). An ultraslow-spreading class of ocean ridge. *Nature*, *426*, 405–412.

Dixon, J., & Dietrich, J. R. (1990). Canadian Beaufort Sea and adjacent land areas. In A. Grantz, L. Johnson, & J. F. Sweeney (Eds.), *The Arctic Ocean region* (pp. 239–256). Boulder, CO: Geological Society of America, The Geology of North America.

Doré, A. G., Lundin, E. R., Gibbons, A., Sømme, T. O., & Tørudbakken, B. O. (2016). Transform margins of the Arctic: A synthesis and re-evaluation. *Geological Society of London Special Publication*, *431*, 63–94. https://doi.org/10.1144/SP431.8

Døssing, A., Jackson, H. R., Matzka, J., Einarrson, I., Rasmussen, T. M., Olesen, A. V., & Brozena, J. M. (2013). On the origin of the Amerasia Basin and the High Arctic Large Igneous Province—Results of new magnetic data. *Earth and Planetary Science Letters*, *363*, 219–230.

Dove, D., Coakley, B., Hopper, J., Kristoffersen, Y., & HLY0503 Geophysics Team. (2010). Bathymetry, controlled source seismic and gravity observations of the Mendeleev Ridge: Implications for ridge structure, origin, and regional tectonics. *Geophysical Journal International*, *183*, 481–502.

Drachev, S. S. (2016). Fold belts and sedimentary basins of the Eurasian Arctic. *Arktos*, *2*, 21–30. https://doi.org/10.1007/s41063-015-0014-8

Ehlers, M., & Jokat, W. (2009). Subsidence and crustal roughness of ultra-slow spreading ridges in the northern North Atlantic and Arctic Ocean. *Geophysical Journal International*, *177*, 451–462. https://doi.org/10.1111/j.1365-246X.2009.04078.x

Engen, O., Faleide, J. I., & Dyreng, T. K. (2008). Opening of the Fram Strait gateway: A review of plate tectonic constraints. *Tectonophysics*, *450*, 51–69. https://doi.org/10.1016/j.tecto.2008.01.002

Embry, A. (2009). Crockerland—The source area for the Triassic to Middle Jurassic strate of northern Axel Heiberg Island, Canadian Arctic Islands. *Bulletin of Canadian Petroleum Geology*, *57*(2), 129–149.

Embry, A., & Dixon, J. (1994). The age of the Amerasia Basin, 1992. Paper presented at proceedings of International Conference on Arctic Margins, Anchorage, AK.

Embry, A. F. (1990). Geological and geophysical evidence in support of the hypothesis of anticlockwise rotation of northern Alaska. *Marine Geology*, *93*, 317–329.

Evangelatos, J., Funck, T., & Mosher, D. C. (2017). The sedimentary and crustal velocity structure of Makarov Basin and adjacent Alpha Ridge. *Tectonophysics*, *696–697*, 99–114. https://doi.org/10.1016/j.tecto.2016.12.026

Evangelatos, J., & Mosher, D. C. (2016). Seismic stratigraphy, structure and morphology of Makarov Basin and surrounding regions: Tectonic implications. *Marine Geology*, *374*, 1–13.

Evenchick, C. A., Davis, W. J., Bédard, J. H., Hayward, N., & Friedman, R. M. (2015). Evidence for protracted High Arctic large igneous province magmatism in the central Sverdrup Basin from stratigraphy, geochronology, and paleodepths of saucer-shaped sills. *Geological Society of America Bulletin*, *127*(9/10), 1366–1390. https://doi.org/10.1130/B31190.1

Freeland, G. L., & Dietz, R. S. (1973). Rotation history of Alaskan tectonic blocks. *Tectonophysics*, *18*, 379–389.

Funck, T., Jackson, H. R., & Shimeld, J. (2011). The crustal structure of the Alpha Ridge at the transition to the Canadian Polar margin: Results from a seismic refraction experiment. *Journal of Geophysical Research*, *116*, B12101. https://doi.org/10.1029/2011JP008411

Gaina, C., Werner, S. C., Saltus, R., Maus, S., & the CAMP-GMGROUP (2011). Circum-Arctic mapping project: New magnetic and gravity anomaly maps of the Arctic. In A. M. Spencer et al. (Eds.), *Arctic petroleum geology* (*Memoirs*, Vol. 35, pp. 39–48). London: Geological Society of London.

Garrity, C. P., & Soller, D. R. (2009). *Database of the Geologic Map of North America—Adapted from the Map by J.C. Reed, Jr., and others (2005)* (USGS Data Series 424). Retrieved from http://pubs.usgs.gov/ds/424/

Gottlieb, E. S., Meisling, K. E., Miller, E. L., & Mull, C. G. (2014). ClosingCanada Basin: Detrital zirxon geochronology relationships between the North Slope of Arctic Alaska and the Franklinian mobile belt of Arctic Canada. *Geosphere*, *10*(6), 1366–1384.

Grantz, A., Clark, D. L., Phillips, R. L., & Srivastava, S. P. (1998). Phanerozoic stratigraphy of Northwind Ridge, magnetic anomalies in the Canada Basin, and the geometry and timing of rifting in the Amerasia basin, Arctic Ocean: GSA. *Bulletin*, *110*(6), 801–820.

Grantz, A., Eittreim, S., & Dinter, D. A. (1979). Geology and tectonic development of the continental margin north of Alaska. *Tectonophysics*, *59*, 263–291.

Grantz, A., Hart, P. E., & Childers, V. A. (2011). A geology and tectonic development of the Amerasia and Canada Basins, Arctic Ocean Chapter 50. In A. M. Spencer et al. (Eds.), *Arctic petroleum geology* (Memoir, Vol. 35, pp. 771–799). London: Geological Society of London. https://doi.org/10.1144/M35.50

Grantz, A., & May, S. D. (1982). Rifting history and structural development of the continental margin north of Alaska. In J. S. Watkins & C. L. Drake (Eds.), *Studies in continental margin geology* (AAPG Memoir 34, 77–100). Tulsa, OK: American Association of Petroleum Geologists.

Grantz, A., May, S. D., & Hart, P. E. (1990a). Geology of the Arctic Continental Margin of Alaska. In A. Grantz, L. Johnson, & J. F. Sweeney (Eds.), *The Arctic Ocean region* (pp. 257–288). Boulder, CO: Geological Society of America, Geology of North America.

Grantz, A., May, S. D., Taylor, P. T., & Lawver, L. A. (1990b). Canada Basin. In A. Grantz, L. Johnson, & J. F. Sweeney (Eds.), *The Arctic Ocean region* (pp. 379–402). Boulder, CO: Geological Society of America, Geology of North America.

Graves, J., Chen, A., Dietrich, J. R., & Dixon, J. (2010). Seismic interpretation and structural analysis of the Beaufort-Mackenzie Basin. *Geological Survey of Canada Open File*, *6217*, 22.

Gürbüz, A. (2010). Geometric characteristics of pull-apart basins. *Lithosphere*, *2*(3), 199–206.

Hadlari, T., Davis, W. J., & Dewing, K. (2014). A pericratonic model for Pearya terrane as an extension of the Franklinian margin of Laurentia, Canadian Arctic. *GSA Bulletin*, *126*(1/2), 182–200. https://doi.org/10.1130/B30843.1

Halgedahl, S. L., & Jarrard, R. D. (1987). *Paleomagnetism of the Kuparuk River Formation from oriented drill core: Evidence for rotation of the Arctic Alaska Plate* (pp. 581–617). Bakersfield, CA: Alaskan North Slope Geology, Pacific Section, SEPM.

Hall, J. K. (1990). Chukchi borderland. In A. Grantz, L. Johnson, & J. F. Sweeney (Eds.), *The Arctic Ocean region* (pp. 593–616). Boulder, CO: Geological Society of America, The Geology of North America.

Harrison, J. C., & Brent, T. A. (2005). Basins and fold belts of Prince Patrick Island and adjacent Areas. Canadian Arctic Islands. *Geological Survey of Canada Bulletin*, *560*, 198.

Harrison, J. C., St-Onge, M. R., Petrov, O. V., Strelnikov, S. I., Lopatin, B. G., Wilson, F. H., . . . Solli, A. (2011). *Geological map of the Arctic* ("A" Series Map 2159A, 9 sheets, 1 DVD). Ottawa, Canada: Geological Survey of Canada. https://doi.org/10.4095/287868

Hegewald, A., & Jokat, W. (2013). Tectonic and sedimentary structures in the northern Chukchi region, Arctic Ocean. *Journal of Geophysical Research: Solid Earth*, *118*, 1–12. https://doi.org/10.1002/jgrb.50282

Helwig, J., Kumar, N., Emmet, P., & Dinkleman, M. G. (2011). Regional seismic interpretation of crustal framework, Canadian Arctic passive margin, Beaufort Sea, with comments on petroleum potential. In A. M. Spencer et al. (Eds.), *Arctic petroleum geology* (Memoir, Vol. 35, pp. 527–543). London: Geological Society of London.

Houseknecht, D. W., & Bird, K. J. (2011). Geology and petroleum potential of the rifted margins of Canada Basin. . In A. M. Spencer et al. (Eds.), *Arctic petroleum geology* (Memoir, Vol. 35, pp. 509–526). London: Geological Society of London.

Houseknecht, D. W., & Connors, C. D. (2015). Mesozoic evolution of the Dinkum Graben, Alaska Beaufort shelf, and petroleum systems implications [Abstract]. *Geological Society of America Cordilleran Sectopm*, T1–10. Retrieved from https://gsa.confex.com/gsa/2015CD/webprogram/Paper255031.html

Houseknecht, D. W., & Connors, C. D. (2016). Pre-Mississippian tectonic affinity across the Canada Basin-Arctic margins of Alaska and Canada. *Geology*, *44*(7), 507–510. https://doi.org/10.1130/G37862.1

Hubbard, R. J., Edrich, S. P., & Rattey, R. P. (1987). Geologic evolution and hydrocarbon habitat of the "Arctic Alaska Microplate." *Marine and Petroleum Geology*, *4*, 2–34.

Hyndman, R. D., Currie, C., & Mazzotti, S. (2005). Subduction zone backarcs, mobile belts, and orogenic heat. *GSA Today*, *15*(2). https://doi.org/10.1130/1052-5173

Ilhan, I., & Coakley, B. (2015). Stratigraphy and structure of the Chukchi Borderland: Implications for the opening of the Canada Basin. Abstract T51B-2875 presented at AGU Fall meeting, AGU, Washington, DC. Retrieved from http://abstractsearch.agu.org/meetings/2015/FM/T51B-2875.html

Ilhan, I., & Coakley, B. (2016). Mesozoic and Cenozoic tectono-depositional history of the southwestern Chukchi Borderland: Implications of pre-Brookian passive-margin slope deposits for the Jurassic extensional deformation of the Amerasia Basin, Arctic Ocean. Paper T32C-02 presented at AGU Fall Meeting, AGU, Washington, DC. Retrieved from https://agu.confex.com/agu/fm16/meetingapp.cgi/Paper/137225

Jakobsson, M., Mayer, L. A., Coakley, B., Dowdeswell, J. A., Forbes, S., Fridman, B., . . . Weatherall, P. (2012). The International Bathymetric Chart of the Arctic Ocean (IBCAO) Version 3.0. *Geophysical Research Letters*, *39*, L12609. https://doi.org/10.1029/2012GL052219

Jokat, W., Kollofrath, J., Geissler, W. H., & Jensen, L. (2012). Crustal thickness and earthquake distribution south of the Logachev Seamount, Knipovich Ridge. *Geophysical Research Letters*, *39*, L08302. https://doi.org/10.1029/2012GL051199

Kandilarov, A., Landa, H., Mjelde, R., Pedersen, R. B., Okino, K., & Murai, Y. (2010). Crustal structure of the ultra-slow spreading Knipovich Ridge, North Atlantic, along a presumed ridge center segment. *Marine Geophysical Researches*, *31*, 173–195. https://doi.org/10.1007/s11001-010-9095-8

Katzman, R., ten Brink, U. S., & Lin, J. (1995). Three-dimensional modeling of pull-apart basins: Implications for the tectonics of the Dead Sea Basin. *Journal of Geophysical Research*, *100*, 6295–6312.

Knudsen, C., Hopper, J. R., Bierman, P. R., Bjerager, M., Funck, T., Green, P. F., . . . Thomsen, T. B. (2017). Samples from Lomonosov Ridge place new constraints on the geological evolution of the Arctic Ocean. In V. Pease & B. Coakley (Eds.), *Circum-Arctic lithosphere and evolution* (Geological Society of London Special Publication 460, 22 pp.). London: Geological Society of London. https://doi.org/10.1144/SP460.17

Kumar, N., Granath, J. W., Emmet, P. A., Helwig, J. A., & Dinkelman, M. G. (2011). Stratigraphic and tectonic framework of the US Chukchi Shelf: Exploration insights from a new regional deep-seismic reflection survey. In A. M. Spencer et al. (Eds.), *Arctic petroleum geology* (Memoirs, Vol. 35, pp. 501–508). London: Geological Society of London.

Lane, L. S. (1997). Canada Basin, Arctic Ocean: Evidence against a rotational origin. *Tectonics*, *16*(3), 363–387.

Lane, L. S., & Dietrich, J. R. (1995). Tertiary structural evolution of the Beaufort Sea-Mackenzie delta region, Arctic Canada. *Bulletin of Canadian Petroleum Geology*, *43*, 293–314.

Lane, L. S., Gehrels, G. E., & Layer, P. W. (2015). Provenance and paleography of the Neurokpuk Formation, northwest Laurentia: An integrated synthesis. *Geological Society of America Bulletin*, *128*(1–2), 239–257. https://doi.org/10.1130/B31234.1

Lawver, L. A., Grantz, A., & Gahagan, L. M. (2002). Plate kinematic evolution of the present Arctic region since the Ordovician. In E. L. Miller et al. (Eds.), *Tectonic evolution of the Bering Shelf–Chukchi Sea–Arctic margin and adjacent landmasses* (Geological Society of America Special Paper 360, pp. 333–358). Boulder, CO: Geological Society of America. https://doi.org/10.1130/0-8137-2360-4.333

Lawver, L. A., & Scotese, C. R. (1990). A review of tectonic models for the evolution of the Canada Basin. In A. Grantz, L. Johnson, & J. F. Sweeney (Eds.), *The Arctic Ocean region, decade of North American geology* (Chap. 31, Vol. L, pp. 593–618). Boulder, CO: Geological Society of America.

Laxon, S., & McAdoo, D. (1994). Arctic Ocean gravity field derived from ERS-1 Satellite Altimetry. *Science*, *265*, 621–624.

Loncke, L., Maillard, A., Basile, C., Roest, W. R., Bayon, G., Gaullier, V., . . . Bourrin, F. (2016). Structure of the Demerara passive-transform margin and associated sedimentary processes. Initial results from the IGUANES cruies. *Geological Society of London Special Publication*, *431*, 179–197.

Lothamer, R. T. (1992). Early Tertiary wrench faulting in the North Chukchi Basin, Chukchi Sea, Alaska. Paper presented at Proceedings of International Conference on Arctic Margins (ICAM). Retrieved from http://www.boem.gov/ICAM92-251/

Maher, H. D. (2001). Manifestations of the Cretaceous High Arctic Large Igneous Province in Svalbard. *Journal of Geology*, *109*, 91–104.

Mann, P. (2007). Global catalogue, classification, and tectonic origins of restraining and releasing bends on active and ancient strike-slip fault systems. *Geological Society of London Special Publication*, *290*(1), 13–142.

Mazzotti, S., & Hyndman, R. D. (2002). Yakutat collision and strain transfer across the northern Canadian Cordillera. *Geology*, *30*, 495–498.

McAdoo, D. C., Farrell, S. L., Laxon, S., Ridout, A., Zwally, H. J., & Yi, D. (2013). Gravity of the Arctic Ocean from satellite data with validations using airborne gravimetry: Oceanographic implications. *Journal of Geophysical Research: Oceans*, *118*, 917–930. https://doi.org/10.1002/jgrc.20080

Miall, A. D. (1976). Devonian geology of Banks Island, Canada Arctic, and its bearing on the tectonic development of the circum-Arctic region. *Geological Society of America Bulletin*, *87*(11), 1599–1608.

Mickey, M. B., Byrnes, A. P., & Haga, H. (2002). Biostratigraphic evidence for the prerift position of the North Slope, Alsaks, and Arctic Ilsands, Canada, and Sinemurian incipient rifting of the Canada Basin. In E. L. Miller, A. Grantz, & S. Klemperer (Eds.), *Tectnoic evolution of the Bering Shelf-Chukchi Sea—Arctic margin and adjacent landmasses* (Geological Society of America Special Paper 360, pp. 67–75). Boulder, CO: Geological Society of America.

Miller, E. L., Gehrels, G. E., Pease, V., & Sokolov, S. (2010). Stratigraphy and U-Pb detrital zircon geochronology of Wrangel Island, Russia: Implications for Arctic paleogeography. *Bulletin American Association of Petroleum Geologists*, *94*(5), 665–692. https://doi.org/10.1306/10200909036

Miller, E. L., Meisling, K. E., Akinin, V. V., Brumley, K., Coakley, B. J., Gottlieb, E. S., . . . Toro, J. (2017). Circum-Arctic lithosphere evolution (CALE) transect C: Displacement of the Arctic Alaska–Chukotka microplate towards the Pacific during opening of the Amerasia Basin of the Arctic. In V. Pease & B. Coakley (Eds.), *Circum-arctic lithosphere evolution* (Geological Society of London Special Publications 460, 64 pp.). London: Geological Society of London. https://doi.org/10.1144/SP460.9

Moore, T. E., & Box, S. E. (2016). Age, distribution and style of deformation in Alaska north of 60oN: Implications for assembly of Alaska. *Tectonophysics*, *691*, 133–170. https://doi.org/10.1016/j.tecto.2016.06.025

Moore, T. E., Wallace, W. K., Bird, K. J., Karl, S. M., Mull, C. G., & Dillon, T. T. (1994). Geology of northern Alaska. In G. Plafker & H. C. Berg (Eds.), *The geology of Alaska* (pp. 49–140). Boulder, CO: Geological Society of America, The Geology of North America.

Mosher, D. C., Chapman, C. B., Shimeld, J., Jackson, H. R., Chian, D., Verhoef, J., . . . Pedersen, R. (2013, May). High Arctic marine geophysical data acquisition. *The Leading Edge*, *2013*, 936–943.

Mosher, D. C., Shimeld, J., Hutchinson, D., & Jackson, R. (2016). *Canadian UNCLOS extended continental shelf program seismic data holdings* (Geological Survey of Canada Open File OF7938). Ottawa, Canada: Geological Survey of Canada. Retrieved from http://geoscan.nrcan.gc.ca/

Mukasa, S., Andronikov, A., Mayer, L. A., & Brumley, K. (2009). Submarine Basalts from the Alpha/Mendeleev Ridge and Chukchi Borderland: Geochemistry of the first intraplate lavas recovered from the Arctic Ocean. *Geochimica et Cosmochimica Acta*, *73*(13), A912.

Naylor, M. A., Mandl, G., & Sijpesteijn, C. H. K. (1986). Fault geometries in basement-induced wrench faulting under different initial stress states. *Journal of Structural Geology*, *8*(7), 737–752.

Nemčok, M., Sinha, S. T., Doré, A. G., Lundin, E. R., Mascle, J., & Rybar, S. (2016). Mechanisms of microcontinent release associated with wrenching-involved continental break-up: A review. In M. Nemčok et al. (Eds.), *Transform margins: Development, controls and petroleum systems* (Geological Society of London Special Publications 431, pp. 323–359). London: Geological Society of London. https://doi.org/10.1144/SP431.14Hubard

Nguyen, N. C., & Mann, P. (2016). Gravity and magnetic constraints on the Jurassic opening of the oceanic Gulf of Mexico and the location and tectonic history of the Western Main transform fault along the eastern continental margin. *Interpretation*, *4*(1), SC23–SC33.

Nikishin, A. M., Malyshev, N. A., & Petrov, E. I. (2014). *Geological structure and history of the Arctic Ocean* (88 pp.). Houten, The Netherlands: European Association of Geoscientists and Engineers.

Nikishin, A. M., Petrov, E. I., Malyshev, N. A., & Ershova, V. P. (2017). Rift systems of the Russian eastern Arctic shelf and Arctic deep water basins: Link between geological history and geodynamics. *Geodynamics and Tectonophysics*, *8*(1), 11–43. https://doi.org/10.5800/GT-2017-8-1-0231

Oakey, G. N., & Saltus, R. (2016). Geophysical analysis of the Alpha-Mendeleev ridge complex: Characterization of the High Arctic Large Igneous Province. *Tectonophysics*, *691*(Part A), 65–84.

O'Brien, T. M., Miller, E. I., Benowitz, J. P., Meisling, K. E., & Dumitru, T. A. (2016). Dredge samples from the Chukchi Borderland: Implications for paleogeographic reconstruction and tectonic evolution of the Amerasia Basin of the Arctic. *American Journal of Science*, *316*, 873–924.

Saltus, R., Miller, E. L., Gaina, C., & Brown, P. J. (2011). Regional magnetic domains of the Circum-Arctic: A framework for geodynamic interpretation, Chapter 4. In A. M. Spencer et al. (Eds.), *Arctic petroleum geology* (Memoir, Vol. 35, pp. 49–60). London: Geological Society of London. https://doi.org/10.1144/M35

Saltus, R. W., & Hudson, T. L. (2007). Regional magnetic anomalies, crustal strength, and the location of the northern Cordilleran fold and thrust belt. *Geology*, *35*(6), 567–570. https://doi.org/10.1130/G23470A.1

Shatsky, N. S. (1935). Tectonics of the Arctic in Geologiya i polyeznye Severa SSSR: Glavsemorputi [in Russian]. *Geologiya*, *1*, 149–168.

Shephard, G. E., Müller, R. D., & Seton, M. (2013). The tectonic evolution of the Arctic since Pangea breakup: Integrating constraints from surface geology and geophysics with mantle structure. *Earth-Science Reviews*, *124*, 148–183. https://doi.org/10.1016/j.earscirev.2013.05.012

Sherwood, K. W. (1994). Stratigraphy, structure, and origin of the Franklinian, northeast Chukchi basin, Arctic Alaska plate. In D. K. Thurston & K. Fujita (Eds.), *Proceedings of International Conference on Arctic Margins* (pp. 245–250). Washington, DC: U.S. Minerals Management Service.

Sherwood, K. W., Johnson, P. P., Craig, J. D., Zerwick, S. A., Lothamer, R. T., Thurston, D. K., & Hurlbert, S. B. (2002). Structure and stratigraphy of the Hanna Trough, U.S., Chukchi Shelf, Alaska. In E. L. Miller, A. Grantz, & S. Klemperer (Eds.), *Tectnoic evolution of the Bering Shelf-Chukchi Sea—Arctic margin and adjacent landmasses* (Geological Society of America Special Paper 360, pp. 39–66). Boulder, CO: Geological Society of America.

Shimeld, J., Li, Q., Chian, D., Lebedeva-Ivanova, N., Jackson, R., Mosher, D., & Hutchinson, D. (2016). Seismic velocities within the sedimentary succession of the Canada Basin and southern Alpha-Mendeleev Ridge, Arctic Ocean: Evidence for accelerated porosity reduction? *Geophysical Journal International*, *204*(1), 1–20. https://doi.org/10.1093/gji/ggv416

Shipilov, E. V., & Lobkovskii, L. I. (2014). The submeridional strike slip zone in the structure of the Chukchi Sea continental margin and the mechanism of opening of the Canada Oceanic Basin. *Doklady Earth Sciencies*, *455*(Part 1), 238–242.

Shipley, T., Gahagan, L., Johnson, K., & Davis, M. (Eds.) (2012). *Seismic Data Center*. Austin, TX: University of Texas Institute for Geophysics. Retrieved from http://www.ig.utexas.edu/sdc/

Sippel, J., Scheck-Wenderoth, M., Lewerenz, B., & Kroeger, K. F. (2013). A crust-scale 3D structural model of the Beaufort-Mackenzie Basin (Arctic Canada). *Tectonophys*, *591*, 30–51.

Smit, J., Brun, J. P., Cloetingh, S., & Ben-Avraham, Z. (2008). Pull-apart basin formation and development in narrow transform zones with application to the Dead Sea basin. *Tectonics*, *27*, TC6018. https://doi.org/10.1029/2007TC002119

Tailleur, I. L. (1973). Probably rift origin of Canada Basin, Arctic Ocean. *AAPG Memoir*, *19*, 526.

Taylor, P. T., Kovacs, L. C., & Vogt, P. R. (1981). Detailed aeromagnetic investigation of the Arctic Basin, 2. *Journal of Geophysical Research*, *86*(B7), 6323–6333.

ten Brink, U. S., Katzman, R., & Lin, J. (1996). Three-dimensional models of deformation near strike-slip faults. *Journal of Geophysical Research*, *101*(16), 16205–16220.

Vogt, P. R., Jung, W.-Y., & Brozena, J. (1998). Arctic margin gravity highs: Deeper meaning for sediment depocenters. *Marine Geophysical Researches*, *20*, 459–477.

Vogt, P. R., Taylor, P. T., Kovacs, L. C., & Johnson, G. L. (1982). The Canada Basin: Aeromagnetic constraints on structure and evolution. *Tectonophysics*, *89*, 295–336.